UTeM

اونيۆرسيتي تيكنيكل مليسيا ملاك

UNIVERSITI TEKNIKAL MALAYSIA MELAKA

Faculty of Electrical and Electronic Engineering Technology

DEVELOPMENT OF OPTICAL MICROFIBER SENSOR FOR CARBON DIOXIDE IN DIFFERENT CONCENTRATIONS USING A TAPERING METHOD

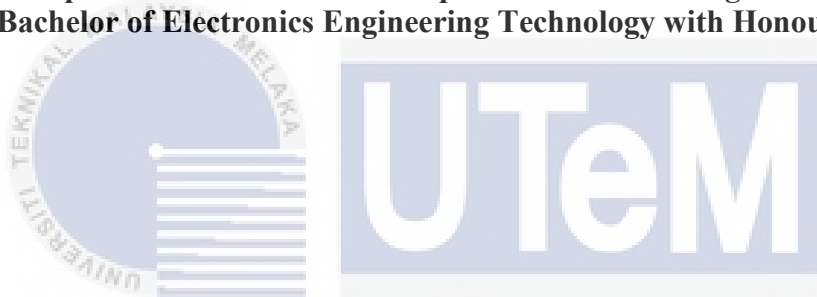**NUR HANIS SURAYA BINTI HASBULLAH**

Bachelor of Electronics Engineering Technology with Honours

2022/2023

DEVELOPMENT OF OPTICAL MICROFIBER SENSOR FOR CARBON DIOXIDE IN DIFFERENT CONCENTRATIONS USING A TAPERING METHOD

NUR HANIS SURAYA BINTI HASBULLAH

A project report submitted
in partial fulfillment of the requirements for the degree of
Bachelor of Electronics Engineering Technology with Honours

Faculty of Electrical and Electronic Engineering Technology

UNIVERSITI TEKNIKAL MALAYSIA MELAKA

2022/2023

DECLARATION

I declare that this project report entitled "Development Of Optical Microfiber Sensor For Carbon Dioxide In Different Concentrations Using A Tapering Method" is the result of my own research except as cited in the references. The project report has not been accepted for any degree and is not concurrently submitted in candidature of any other degree.

Signature	:	
Student Name	:	NUR HANIS SURAYA BINTI HASBULLAH
Date	:	31 DECEMBER 2022

APPROVAL

I hereby declare that I have checked this project report and in my opinion, this project report is adequate in terms of scope and quality for the award of the degree of Bachelor of Electronics Engineering Technology with Honours

Signature :

Supervisor Name : DR. AMINAH BINTI AHMAD

Date : 31 DECEMBER 2022

Signature :

Co-Supervisor :

Name (if any) : DR. MD ASHADI BIN MD JOHARI

Date : 31 DECEMBER 2022

DEDICATION

My special thanks go to my parents, siblings, and friends, who have always supported me and encouraged me to complete my final year project successfully. Meanwhile, I'm dedicating this thesis to my beloved supervisor, Dr. Aminah binti Ahmad, and co. supervisor Dr. Md Ashadi bin Md Johari who has given me a lot of guidance on how to achieve success for my final year project. Thank you very much. It means a lot to me. I am grateful for their inevitable sacrifice, tolerance, and consideration in making this effort feasible. I cannot provide the appropriate words that can accurately describe my appreciation for their loyalty, support, and belief in my ability to achieve my dreams.

ABSTRACT

Fiber optics, commonly referred to as optical fiber, is a medium and system for transmitting information as light pulses over a glass or plastic strand. When light signals are transmitted through fiber optic cable, they bounce off the core and cladding in a sequence of zig-zag bounces, a phenomenon known as total internal reflection. Recently, optical microfiber sensors have received considerable research efforts due to their high sensitivity, detection speed, high flexibility and low optical power consumption. This research will focuses on the optimisation performance of tapered silica microfiber as an sensing platform. The microfiber optics sensor were developed to detect the concentrations of different CO_2. The objective of this project was to use microfiber optics as a sensor to detect carbon dioxide (CO_2) using a tapering method. Furthermore, the reduced diameter of the tapered section of the optical microfiber can be beneficial when measuring physical parameters. This project requires an understanding, development and analysis on different concentrations of CO_2 sensors from optical loop microfibers and needs to know how to perform microfiber splicing, cutting, stripping and methods used. There will be five samples of different concentrations of CO_2 tested. The experimental findings will be described in terms of sensitivity, correlation, and graphical determination coefficients, all of which depend entirely on the CO_2 concentration and the light source. At the end of the project, an optical microfiber different concentration sensor with high sensitivity readings was formed. Next, the results were analysed using the factorial design method. This will determine which samples of different CO_2 concentrations that has the optimum performance in terms of concentration.

ABSTRAK

Gentian optik, biasanya dirujuk sebagai gentian optik, ialah medium dan sistem untuk menghantar maklumat sebagai denyutan cahaya ke atas helai kaca atau plastik. Apabila isyarat cahaya dihantar melalui kabel gentian optik, ia melantun dari teras dan pelapisan dalam urutan lantunan zig-zag, fenomena yang dikenali sebagai pantulan dalaman total. Baru-baru ini, penderia mikrofiber optik telah menerima banyak usaha penyelidikan kerana kepekaan yang tinggi, kelajuan pengesanan, fleksibiliti tinggi dan penggunaan kuasa optik yang rendah. Penyelidikan ini akan memberi tumpuan kepada prestasi pengoptimuman mikrofiber silika tirus sebagai platform penderiaan. Sensor optik mikrofiber telah dibangunkan untuk mengesan kepekatan CO_2 yang berbeza. Objektif projek ini adalah untuk menggunakan optik mikrofiber sebagai sensor untuk mengesan karbon dioksida (CO_2) menggunakan kaedah tirus. Tambahan pula, diameter kecil bahagian tirus mikrofiber optik boleh memberi manfaat apabila mengukur parameter fizikal. Projek ini memerlukan pemahaman, pembangunan dan analisis tentang kepekatan berbeza penderia CO_2 daripada mikrofiber gelung optik dan perlu mengetahui cara melakukan penyambungan, pemotongan, pelucutan dan kaedah yang digunakan. Akan ada lima sampel kepekatan CO_2 yang berbeza diuji. Penemuan eksperimen akan diterangkan dari segi kepekaan, korelasi, dan pekali penentuan grafik, yang semuanya bergantung sepenuhnya pada kepekatan CO_2 dan sumber cahaya. Pada akhir projek, sensor kepekatan berbeza mikrofiber optik dengan bacaan kepekaan tinggi telah dibentuk. Seterusnya, keputusan dianalisis menggunakan kaedah reka bentuk faktorial. Ini akan menentukan sampel kepekatan CO_2 yang berbeza yang mempunyai prestasi optimum dari segi kepekatan.

ACKNOWLEDGEMENTS

iii

TABLE OF CONTENTS

LIST OF TABLES

LIST OF FIGURES

LIST OF SYMBOLS

θ_1	-	The incident angle between the light beam and the normal
θ_2	-	The refractive angle between the light ray and the normal
n_1	-	The refractive index of the medium the light is leaving
n_2	-	Refractive index of the material the light is entering
v_1	-	is the speed of light at the first medium
v_2	-	is the speed of light at the second medium
λ	-	Wavelength
μm	-	Micrometer
nm	-	Nanometer
ηEF	-	Fraction of power
λ/r	-	Normalized wavelength
$\sqrt{}$	-	Square root
R^2	-	Coefficient of determination

LIST OF ABBREVIATIONS

CO_2	-	Carbon dioxide
dBm	-	Decibels per milliwatts
EMI	-	Electromagnetic interference
SMF	-	Single mode fiber
RI	-	Refractive index
FBG	-	Fiber bragg gratings
LPG	-	Long period grating
PCF	-	Photonic crystal fiber
MF	-	Microfiber
MMF	-	Multimode fiber
MCR	-	Microfiber coil resonator
MLR	-	Microfiber loop resonator
MKR	-	Microfiber knot resonator

LIST OF APPENDICES

CHAPTER 1

INTRODUCTION

1.1   Background

Optical fiber were widely used in the field of telecommunications during the last century due to their special features, such as low transmission loss, high bandwidth, and multiplexing capability. Optical fiber applications have recently shifted to other areas such as sensing to take advantage of its unique properties. Despite the fact that established electronic sensors have lower prices, optical sensors may be able to find a target application by utilising their unique features. Low losses, remote sensing, immunity to electromagnetic interference, no electrical biassing is required to guide light, and the ability to use in an explosion risk environment are some of the special features.

Currently, optical fiber sensors are being pursued for a variety of bio-chemical sensing applications, including ethanol, sodium hypochlorite, formaldehyde, and human chorionic gonadotropin. It is driven by the rapid development of micro or nanotechnology and the need to reduce sensor size while maintaining the key requirements of the sensor such as low power consumption, faster response, better spatial resolution, and higher sensitivity.

Microfibers have unique features such as large optical confinement, configurability, flexibility, strong optical confinement and a large evanescent field, which make them ideal for physical sensing applications such as ultra-sensitive surface absorption spectroscopy, hydrogen detection, chemical and refractive index sensors. It is extremely sensitive to changes in the ambient refractive index because of the large evanescent wave propagating outward from the microfiber. The refractive index of the surrounding material rises as the

proportion of power transmitted in the evanescent field increases. It has good evanescent coupling with metal, semiconductor, and substrate waveguides.

The purpose of this study is to develop the optical microfiber sensor to detect Carbon dioxide (CO_2) using a tapering method. An SMF28 optical cable or fiber optic pigtail under test, a laser source with a wavelength of 1550nm, an Optical Power Level and Optical Power Meter, and five samples of different concentrations of CO_2 are required for this project. There will be five samples of different concentrations of CO_2 tested, with the results being the loss (dBm) at the peak of the spectrum obtained with the Optical Power Level and Optical Power Meter equipment. The outcome of the experiment will be described in terms of sensitivity, correlation, and graph coefficient of determination, all completely dependent on the CO_2 concentration and light source.

1.2   Problem Statement

The purpose of this study is to analyse the performance of microfiber optics as a gas sensor in detecting CO_2 of three different concentrations using a tapering method. Human activities such as deforestation, coal and tree combustion have increased the concentration of CO_2 in the atmosphere. CO_2 concentrations are rising because of the fossil fuels that people use for energy. According to studies, human activities contribute up to 110.5 million tons of CO_2 to the atmosphere every day [1]. The carbon dioxide at a normal level will not show more impact on the environment. However, when it increases due to some human activities, it will show more impact on global warming. Too much carbon dioxide can also be harmful to one's health. This includes dizziness, headaches, restlessness, difficulty breathing, tiredness, and increased heart rate. For each different concentration of CO_2 gas released has its own results of the concentration, thus it will determine the reading value due to the different concentrations of CO_2 at the highest sensitivity.

2

Next, there are numerous sensors available for measuring of different concentration, particularly when employing electronic devices. Despite the fact that electronic sensors perform well in practise, they are not user-friendly due to their flammability due to electromagnetic interference (EMI). This difficulty can be remedied by utilising a microfiber optic sensor composed of silica glass, which is EMI resistant. During the monitoring procedure, it solely employs light pulses to send the signal. As a result, no EMI from the environment will impair its performance.

Besides, to monitor the different concentration, the electronic sensor requires a large amount of power. The cost of employing a microfiber optic sensor, on the other hand, can be decreased because it only requires a tiny amount of electricity to provide the optical power source for detection. Therefore, the idea development of microfiber optic sensor is to determine which measurements require a low or high sensitivity. As a result, an optical microfiber sensor will be used in this investigation to analyse and check the performance of five different samples of concentrations using a tapering method.

1.3   Project Objective

The objectives are stated as below:

a)   To study microfiber optics as a gas sensor to detect Carbon dioxide (CO2).

b)   To develop the microfiber optics as a gas sensor to detect Carbon dioxide (CO2) using atapering method.

c)   To analyse the performance of microfiber optics as a gas sensor in detecting Carbon dioxide (CO2).

3

1.4   Scope of Project

Scope of this project mainly focused on develop the microfiber optics as a gas sensor to detect carbon dioxide (CO2) using a tapering method. The performance of the developed sensors will also be evaluated. A coating length of several cm is removed from the Single Mode Fiber (SMF) to fabricate tapered fiber. Then, microfiber optic sensor is spliced using a commercial splicer Fujikura FSM-18R. The fibers are cleaned with alcohol to remove dust and cleaved with a Fujikura CT-30 Fiber Cleaver to obtain a smooth cleavage surface and clean end-uncoated fiber before the sensors are spliced. The 1550nm input wavelength was collected from an Optical Power Level source during the testing process, and the output signal was measured in (dBm) units using an Optical Power Meter.

Next, the splicer connects the two fiber optics by splicing the sensors together. Then, for each microfiber optic sensor, an Optical Power Level supply and an Optical Power Meter are connected to detect and analyse different concentrations of CO2. Furthermore, three samples of different concentrations of CO2 are ready to be placed into airtight container. As a result, there are four processes in this project for testing the different concentration of CO2. The tapered silica microfiber is tested using the sensors created as part of this project. By utilising an Optical Power Meter, the findings are converted to watts (dBm). This project gurantees that the project is moving in the right path to achieve its objectives.

Table 1.1 Equipment used during this project

Equipment	Experiment Details
Airtight plastic container	Used to trap the CO2 through the experiment
Microfiber optic	Single mode fiber (1550nm)
Gas	Carbon dioxide (CO2)

Impra board	To lay the tapered silica fiber
Straw	The medium used to released the CO2 gas through respiration into the airtight plastic container that containing tapered silica microfiber
Plasticine	The medium used to tightly compress the airtight container so that no air can get in or out
Hardware	Optical Power Meter Optical Power Level/Source (1550nm) Commercial Splicer Fujikura FSM-18R Fujikura CT-30 Fiber Cleaver

CHAPTER 2

LITERATURE REVIEW

2.1   Introduction

Optical fiber endoscopes were most likely the first commercially available fiber-optic sensors in the early 20th century [1] [2]. These devices have and continue to revolutionized medicine. Modern fiber optic sensors are made with recently developed ultralow-loss silica optical fibers. Thus, fiber-optic sensors have experienced rapid development as a result of their many benefits, including their resistance to electromagnetic interference, multiplexed or distributed sensing, large operation bandwidths, light weight, biocompatibility and endurance in harsh environments. A glass core with a high refractive index (RI) is typically surrounded by cladding materials with a lower refractive index in optical fiber configurations. The interactions between light and its environment are very weak because light is tightly contained in the optical fibers core region. Most of the early fiber-optic sensing systems, such as the interferometric-based hydrophones and the fiber optic gyroscope, required a sufficient length of optical fiber in order to sense the weak environmental perturbations.

In optical fibers and fiber-optic sensors, microstructures have opened up a new era. Optical communication systems were the first to use one-dimensional (1D) photonic crystal structures like fiber Bragg gratings (FBGs). Because they can measure physical parameters absolutely and independently of a reference, and because they can withstand system fluctuations, FBGs have been found to be superior fiber-optic sensors. After the FBG, different various grating structures are produced, including the chirped fiber Bragg grating, long period grating (LPG), and tilted-FBG. In addition, they demonstrate a variety of sensing

6

abilities that nicely complement the benefits of FBG-based sensors. Photonic crystal fibers (PCF) were created by combining optical fibers and two-dimensional (2D) photonic crystals. The PCFs can implement lab-on-fibers by enabling light-matter interactions at the microscale in their hollow channels PCFs have been widely used in photochemistry, gas and liquid phase chemical sensing, and other fields

Another rapidly evolving fiber-optic sensor type with a crucial need for micro or nanophononics is the optical microfiber (MF). It is expected that reduction sensing structures will result in better performance, power, volume, and cost. The diameter of MF is between tens of nanometers and micrometers smaller than that of standard optical fiber. As a result of the light diffraction limit for subwavelength scale MF, a significant portion of the evanescent field of MF is allowed into the environment, giving MF the capacity to interact strongly with its surroundings. The MF has also been widely used in optical sensors, evanescent field coupling, particle trapping or manipulating, and quantum optics. The MF demonstrates good flexibility to realize different microstructures as effective sensing heads, such as loop, knot, coil, and optical coupler. This is made possible by their good flexibility and mechanical strength. Additionally, nonlinear optics are intrigued by the strong field confinement and tunable dispersion of MF.

Various techniques for fabricating the MF have been proposed throughout the evolution of MF research, depending on the precursor materials or optical fibers. The flame heating-pulling method was first reported to draw MFs with a thickness of several micrometers from standard optical fiber. Tong et al. introduced a two-step drawing method to fabricate silica MF with atomic surface smoothness down to 50 nm. The configurations of the flame tapering system were improved by Brambilla et al. who also demonstrated subwavelength silica MF with a loss of less than 0.01 dB/mm.
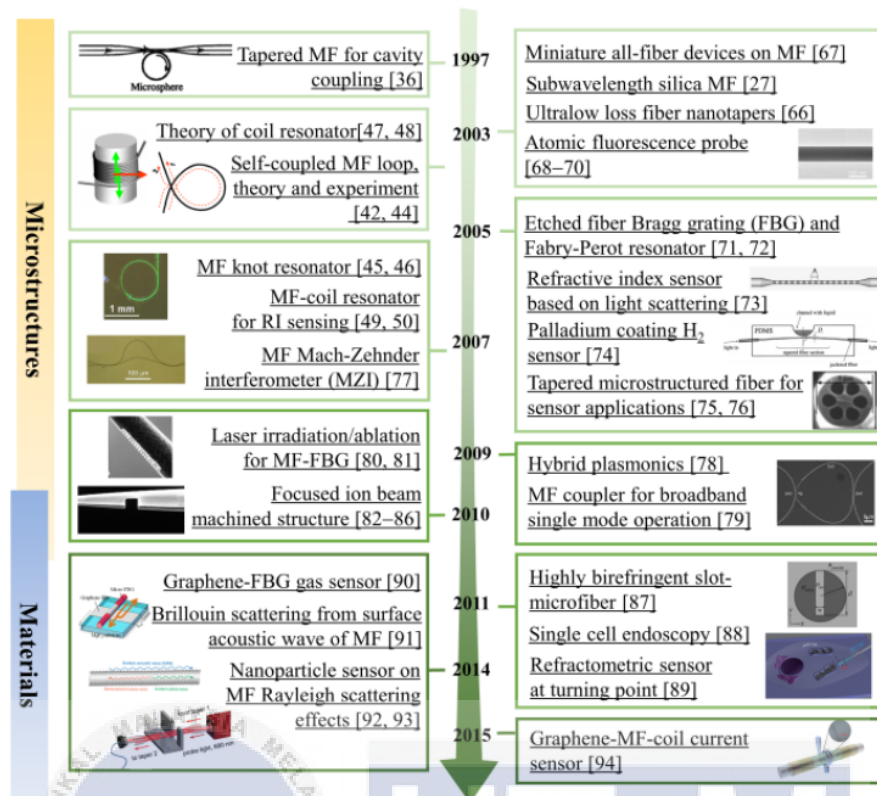
Figure 2.1 A brief summary of silica microfiber optical sensors (1997-2015) **[3].**

Additionally, they provided a method for fabricating MF using compound glass fiber. In order to fabricate silica MF, Sumetsky et al. reported using indirect CO_2 laser heating method to fabricate silica MF. A hydrofluoric acid flow etch technique was described by Zhang et al. for fabricating low-loss, subwavelength MF. Directly drawing from bulk glass or polymer solutions was a different method of getting to MF. Rapid developments in MF-based optical sensors have been seen in recent years. Even though many significant works have been published, only a few of the representative events are shown in Figure 2.1.

2.2   Optical Microfiber

Microfiber optics have special characteristics that include large optical confinement, customizable, flexibility, strong optical confinement, and a large evanescent field. They are suited for applications requiring physical sensing such a surface absorption

spectroscopy with high sensitivity, hydrogen detection, chemical and refractive index sensors [4]. Because of their sensitivity to changes in the ambient refractive index, large evanescent waves propagate out of microfiber. The refractive index of their surrounding material increases as the proportion of power transmitted part in the evanescent field increases. It has a good evanescent coupling with other waveguides including metal, semiconductor, and also the substrate. Therefore, a high fractional evanescent field allow a great response towards humidity sensing.

The physical characteristics of the fiber, such as RI, core diameter, and operating wavelength, could determine the type and number of modes propagating through it. The majority of light energy is contained within the fiber, while some enters the clad. The small portion decays exponentially into the edge of the core-cladding. The low amplitude of the evanescent field in a normal single mode fiber (SMF) could be increased by tapering in order to increase analyte interaction with the transmitted light around the taper region.

2.2.1   Single Mode Fiber

SMF has a small core diameter of 8 to 9 μm and a coating diameter of 125 μm, as shown in Figure 2.2. Therefore, the ratio of core to cladding is usually equal to 9:125.
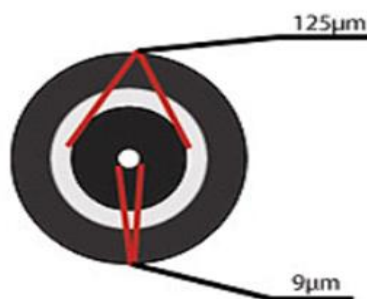
Figure 2.2 Single mode core and cladding measurement **[5].**

Due to the narrow core design, it only allows one light scattering band, as shown in Figure 2.3 [6] below.
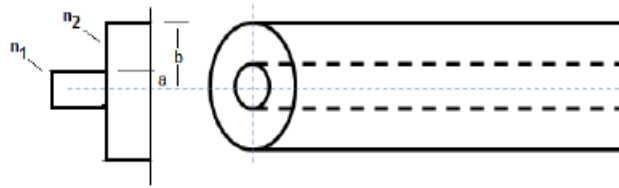
Figure 2.3 Step-index single mode **[7].**

The advantage of having a narrow diameter is that light can move farther with low damping because low light reflection occurs when passing through the core. Therefore, it has lower data loss and better data transmission capabilities, making it suitable for communication. It can transmit up to 40 GB of information within hundreds of kilometers, with a lower data loss rate and faster than MMF.

However, due to the limited mechanical tolerances of the connection with the connector, the narrow SMF core is difficult to insert the light into the core. As a result, it is more difficult to construct. Therefore, its cost is more expensive than MMF.

2.2.2   Total Internal Reflection

The principle of total internal reflection is used to guide light through fibers. The critical angle of occurrence is the angle at which the amount of internal reflection occurs [8]. According to Figure 2.4, when the incident angle exceeds the critical angle, light continuously reflects inside the core and cannot escape. Light normally propagates in a straight line, but light reflections occur when the phase of light changes due to changes in the degree of freedom. When an unexpected phase shift or phase break occurs at the interface of two mediums, light reflection and refraction occur [7].
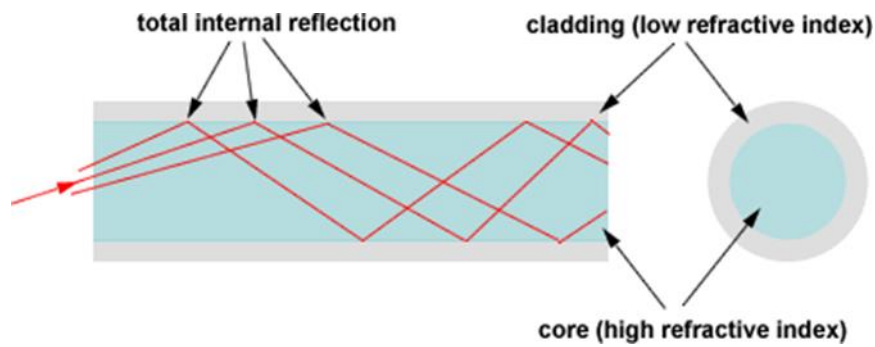
Figure 2.4 Total internal reflection inside the core **[9].**

Total internal reflection happens when a propagating wave strikes a medium barrier at an angle greater than a specific critical angle with respect to the normal surface. For example, if the refractive index on the other side of the boundary is less than the critical angle and the incidence angle is greater than the critical angle, the wave cannot pass through. The critical angle is defined as the incidence angle above which the entire internal reflectance is visible. Aside from that, light refraction happens when a light beam changes direction as it passes from one transparent substance to another.

2.2.3   Snell's Law Concept

Snell's law outlines the connection between incident angle and refracted light angle at two distinct media interfaces. According to Snell's law, the ratio of incidence and refractive angles is identical to the ratio of phase velocities in the two mediums. Therefore, it is also equivalent to the reciprocal of the refractive index ratio.

11

$$n_1 \sin \theta_1 = n_2 \sin \theta_2$$
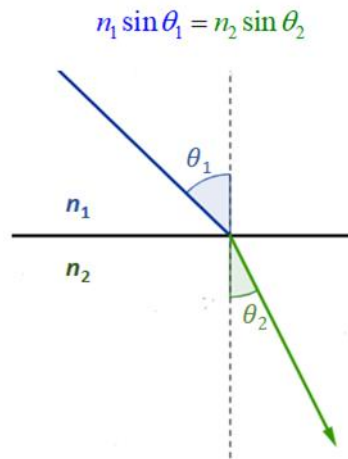
Figure 2.5 Snell's law concept **[7].**

Based on the figure 2.12. Snell's law can be expressed as;

$$\frac{\sin \theta_1}{\sin \theta_2} = \frac{n_2}{n_1} \ or \ \frac{\sin \theta_1}{\sin \theta_1} = \frac{v_1}{v_2} \tag{2.1}$$

Where: θ_1 is the angle of incidence

θ_2 is the angle of refraction

n_1 is an index of the first medium

n_2 is an index of the second medium

v_1 is the speed of light at first medium

v_2 is the speed of light at second medium

    The angle of refraction can be calculated using Equation 2.1 and the refractive indices of the two media. The angle of refraction will be smaller if the second medium's refractive index is greater than the first medium's, and vice versa.

2.3 Types of Optical Fiber

Fiber optic cables use an optical power source to transmit information to an output such as an optical power meter or an optical spectrum analyzer. Fiber optic cables are widely used for environmental monitoring because they offer numerous advantages over traditional electronic sensors. Because of its small size and cylindrical geometry, it is easily assembled into various structures such as composite materials with little interference. Second, the optical fiber is immune to EMI, which is flammable and hazardous to the environment. In addition to its light and high sensitivity, it is also more resistant to harsh environments such as very high and low temperatures, vibration, radiation, pressure, and corrosive conditions [10]. Optical fibers are classified into two types which plastic optical fibers and glass optical fibers. The type of optical fiber used depends on the application.

2.3.1 Plastic Optical Fiber

Plastic optical fibers are typically made with the core material polymethyl methacrylate (PMMA) and the coating material silicone resin. It produces red and green light that is safe for the eyes and can be installed at home without endangering people. There are several advantages and disadvantages to using plastic fibers. One of the benefits of plastic optical fiber is that it comes in a variety of diameters ranging from 0.15mm to 20mm. Furthermore, it is more flexible and can be bent without cracking or breaking. It can also withstand vibrations and unstable environments. These features make it suitable for use in automotive and industrial lighting. It also has lower material costs and a more complicated manufacturing process.

Some disadvantages make it less desirable than glass optical fibers. First, it has a narrower numerical range of 0.48 to 0.63. As a result, it has a low light accumulation

capability, allowing it to capture less light. Next, it cannot withstand harsh environments, and the fibers deteriorate quickly.

Figure 2.6 Plastic optical fiber **[11].**

2.3.2   Glass Optical Fiber

Glass optical fibers are typically made of pure glass or silica as the core material, and less pure glass or plastic as the coating material. It has several advantages over plastic optical fibers. The first benefit is a larger numerical aperture, which allows more light into the system from 0.25 to 1. The second advantage is that it can withstand temperatures as low as -40F and as high as +900F. As a result, it is beneficial and can be used in a variety of applications such as ovens, machines, and cold storage. The third advantage is that it can transmit a wider spectrum of light, including ultraviolet (UV), visible, and infrared (IR) light. The fourth advantage is that it can adapt to wet and corrosive environments without losing performance.

14

Figure 2.7 Glass optical fiber **[11].**

Unfortunately, it has some disadvantages, such as being limited to diameter measurements ranging from 0.05 mm to 0.15 mm and being more brittle and easily broken if not handled carefully. It is also more difficult to handle and finer than plastic optical fibers. As a result, the cost of implementing glass fiber optics is more expensive.

Table 2.1 Comparison between plastic and glass optical fibers

Consideration	Plastic Optical Fiber	Glass Optical Fiber
Cost	Cheaper	More expensive
Transfer speed	Slower	Faster
Loss	Higher Losses	Lower Losses
Numerical Aperture	Lower	Higher
Temperature	Not suitable for extreme temperature	Able to withstand extreme temperature
Flexibility	More flexible	More fragile
Distance	Used for shorter distance	Use for longer distance

2.4   Properties of Optical Microfiber

Microfiber has several intriguing optical properties, including a strong evanescent field. At the outer physical boundary of the small radii microfiber, fractional power spreads in the evanescent field. This property is required for the fabrication of high quality factor (Q) resonators and the beginnings of light into high Q microresonators. Microfiber also has a strong near-field interaction with its surroundings. It has a good evanescent coupling between the microfiber and other waveguides like substrates, semiconductors, and planar waveguides. This tends to result in an abundance of optical devices such as resonators, sensors, and lasers.

Propagation loss is another important property of microfiber. Cracks, impurities connected to the micro or nano fiber surface, and surface imperfections are all causes of propagation loss. It increases as the microfiber radii decrease. Theoretical studies on non-adiabatic intermodal transitions were established to examine the minimum microfiber waist diameter that can propagate signal. The transmission mode would vanish at a rate approximately equal to the radiation wavelength. It was also discovered that when there is a generation of cracks at the facet due to water absorption, the small size microfiber degrades faster in air.

Furthermore, due to its small mass, microfiber is extremely sensitive to momentum changes of photon guides caused by mechanical displacement or vibration mass. This allows for the development of small optomechanical components and devices. It also allows for low loss when passing light through sharp bends. As a result, microfiber could be used to create compact devices with lower power consumption, faster response, and smaller footprints. Microfiber is formed by extending optical fibers until they reach the desired waist diameter while maintaining the original fiber sizes at their input and output ends. This facilitates low-loss splicing with other standard-size optical fibers. It could also be bent with a small bending

radius to produce compact devices. The small waist fiber also transmits a large fraction of the power outside the microfiber and overlaps with the external elements. Any changes in the surrounding properties result in a change in output, as shown in Figure 2.8 [12].
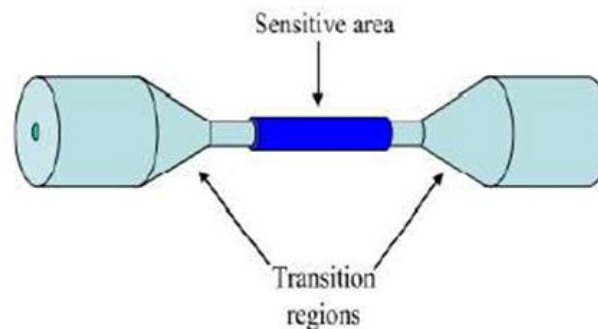
Figure 2.8 Sensitive area with a large fraction of power propagating to interact with their surroundings **[12].**

2.5   Microfiber Fabrication Techniques

Tapering an SMF is the process of reducing the diameter of the cladding (along with the core) by pulling the fiber's end while heating the fiber's waist. Light propagates inside the core infiltrates the cladding during the tapering process. As an outcome, they act as a new core, and the external element uses as a new cladding. Surface smoothness and geometric uniformity during the microfiber fabrication procedure are critical for achieving a high signal-to-noise ratio and low optical loss criteria.

If the majority of the power decouples from higher order modes and remains in the fundamental mode as the power propagates along the taper, the tapered fiber meets adiabatic criteria. It is possible to demonstrate it by demonstrating a tiny taper angle to the relative local change of the taper radius. When the fiber is pulled during the tapering process, its radius decreases and light extrudes from the core to the cladding, propagating throughout the taper region. The mode would thus be influenced by the core, cladding, and air. The shape of the taper has a strong influence on mode evolution inside a tapered fiber or

17

microfiber. When the taper is too steep, non-adiabaticity occurs, resulting in low transmission. When the tapering angle is reduced, mode propagation becomes more adiabatic. Figure 2.10 (i) illustrates the shape differences between adiabatic and non-adiabatic tapered fibers. There are several tapering methods to fabricate the glass microfiber, including self-modulated taper drawing, flame brushing and direct drawing from the bulk technique.

Aside from the tapering method, heat sources are also important in producing high-quality microfiber. Flame, fusion splicer, CO_2 laser beam, and micro furnace are four common heat sources used during the tapering process. The first canonical segment occurred relatively at the long taper waist segment, where the fiber gradually decreases into a small and uniform diameter. The waist is the second conical segment, which merges into the original SMF size. Controlling pulling settings such as pulling speed, heated zone length, and pulling temperature allowed the tapered fiber to be formed into various properties and shapes. The most common heated source is flame-heated. Under a specific pulling force, the fiber is slowly elongated and stretched. At the fiber's center, a hydrogen flame is used. The process is repeated until the desired diameter or length is reached. The propagation loss, group velocity delay, and multimode interference of the microfiber waveguides could be monitored during the tapering process.

The disadvantage of the conventional flame-heated technique is the random turbulence of the oxygen and flame during the burning process. As a result, CO_2 lasers have been developed to solve this problem. Direct laser heating provides a self-regulating control in which the stretching process stops when the fiber diameter reaches a desired value. Electrically heated taper drawing is another technique. By precisely controlling the temperature distribution, this technique can shape the fiber into various geometries. It also provides an effective method for drawing microfiber with greater flexibility.

2.5.1 Self-modulated taper drawing

The first technique is selfmodulated taper drawing. It is a two-step process. First, the waist diameter of the single mode fiber is reduced to a micro-meters using a standard flame brushing technique. The microfiber is then broken into two parts, and one of the fiber pigtails is enfolded onto a small hot sapphire rod, and the microfiber is further drawn to sub-micron diameter. Following that, the sapphire tip is heated using a flame at a distance from the fiber to stabilize the temperature distribution and trap the heat in a small volume.

2.5.2 Flame brushing technique

The second method is flame brushing, as shown in Figure 2.10 (ii). This technique was developed initially to manufacture couplers. It is conducted by applying a small flame movement under a stretched optical fiber. The optical fiber extremities and burner are hold by stages and connected to the computer. By precisely controlling the flame movement, a highly accurate microfiber could be formed. It was able to produce micro or nanofibers with radius as small as 30 nm and longest nanowires with lesser measured loss. Furthermore, this technique allows the microfiber to have both ends pigtailed, which is essential in practical applications with connectivity issues.

The flame brushing technique has been improved to become the modified flame brushing technique. The technique is similar to the conventional flame brushing technique, but the flame is changed with a different heat source, which is a micro-heater or a sapphire capillary tube heated by a CO_2 laser beam. A resistive element that allows temperature to be adjusted by altering the current level is referred to as a micro-heater. Temperature control with a sapphire or CO_2 can be adjusted by changing the degree of focusing of the laser beam onto the sapphire tube. This technique is superior in terms of processing temperature for producing a wide range of low softening microfibers.

2.5.2.1 Adiabaticity Criteria

Tapered fiber is made by stretching a heated conventional single-mode fiber (SMF) to form a structure to reducing a core diameter. The waist is the smallest diameter part of the tapered fiber, as shown in Figure 2.9. Transition regions exist between the uniform unstretched SMF and the waist, with cladding and core diameters decreasing from the rated size of SMF to the order of micrometer or even nanometer. The field distribution varies with the change in core and cladding diameters as the wave propagates through the transition regions. The propagating wave may experience a certain level of energy transfer from the fundamental mode to a few nearby higher order modes, which are most likely to be lost, as a function of the rate of diameter change of any local cross section. The accumulation of this energy transfer along the tapered fiber may result in significant through loss. This excess loss can be reduced if the shape of the fabricated tapered fiber adheres to the adiabaticity criteria throughout.

Figure 2.9 Profile diameter of a tapered fiber **[13]**

2.5.3 Direct drawing from the bulk technique

A small sapphire rod was heated and placed in contact with bulk glass for this technique. This results in localized softening of the bulk glass. Micrometric glass filament is formed when the sapphire rod is abruptly removed [14]. It has the advantage of flexibility and low-cost equipment. However, maintaining the uniformity and diameter of the

microfiber is extremely difficult. It is widely used to fabricate the microfibers from phosphate, tellurite, and polymers
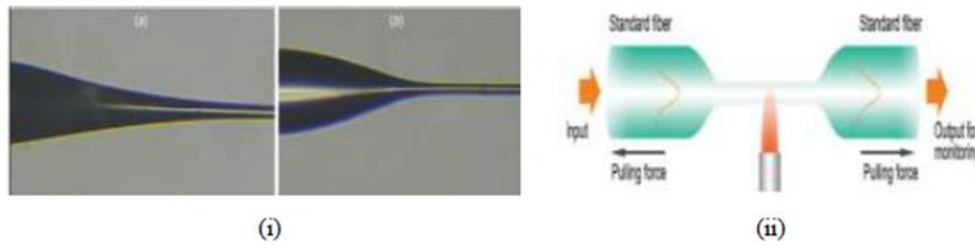
Figure 2.10 (i) Image of microscopic; (a) Adiabatic tapered fiber and (b) Non-adiabatic tapered fiber, (ii) microfiber fabrication technique using a flame heated source **[15].**

2.6 Optical Sensor using Microfiber

Microfiber has unique properties such as visible surface field amplification, a strong evanescent field, huge waveguide dispersion and configurability, which opens up exciting possibilities for sensing applications. Microfiber has high evanescent coupling with other waveguides such as metal, semiconductors, and substrates, as well as near-field interaction with its surroundings. A large evanescent field is an essential criteria for sensing applications where a significant power fraction is required to interact with the surrounding refractive index medium [16].

2.6.1 Evanescent Wave

A standard silica fiber is divided into two main parts which is core and cladding. Core commonly has higher refractive index (RI) to guarantee total internal reflection (TIR) under certain conditions according to Snell law. Nonetheless, a small portion of energy transmission is always coupled into the cladding modes, which is known as the evanescent field. Evanescent wave is electromagnetic field loss that represents a small portion of energy that penetrates the edge of the core and cladding medium during TIR. TIR occurs when the

21

incident angle (θi) is greater than the critical angle (θc), causing light to reflect back from the core to the cladding surface.

According to research, the fraction of power in the evanescent field increases as the normalized wavelength (λ/r) and surrounding refractive index increase. Due to Figure 2.11, the fraction of power (ηEF) is affected by the (λ/r) ratio. When λ/r increases, ηEF increases monotonically. As a result, a microfiber with a smaller radius would have a larger evanescent wave fractional power. When the diameter of the fiber is comparable to the wavelength, a fraction of power propagates in the evanescent field. The evanescent field interacts with any environmental change, making it suitable for sensing applications.
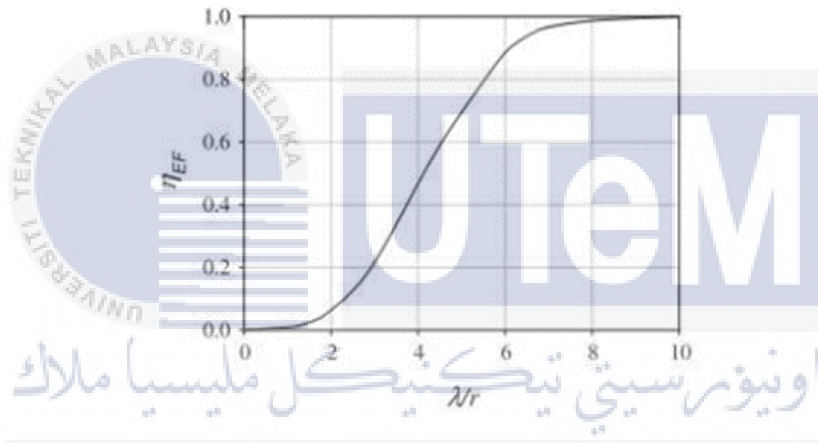
Figure 2.11 Relationship between fraction of power (ηEF) of the silica microfiber and the normalised wavelength (λ/r) (**[17]**).

2.5.2 Optical Microfiber Resonators (OMR_S)

Microfiber can be used to manufacture various resonant structures such as micro-loops, micro-knots, and micro-coils, as well as to excite resonant modes such as microspheres, micro-disks, microcapillaries, and microbottles. This would result in modes propagating between two adjacent large evanescent field sections, which would overlap and couple to produce a compact resonator. The most important parameter in a resonator is the

quality factor Q. It can be calculated by dividing the wavelength λ by the bandwidth (FWHM) of a resonance in the transmission spectrum, as shown in (2.2).

$$Q = \frac{\lambda}{FWHM}$$ (2.2)

Vienna et al. also mentioned that he used loop and knot resonators as refractometric sensors that operate by utilizing a significant fraction of the microfiber mode that transmits in the fluidic channel. Any variation in the analyte refractive index would results in a resonant wavelength shift, as seen in Figure 2.12.
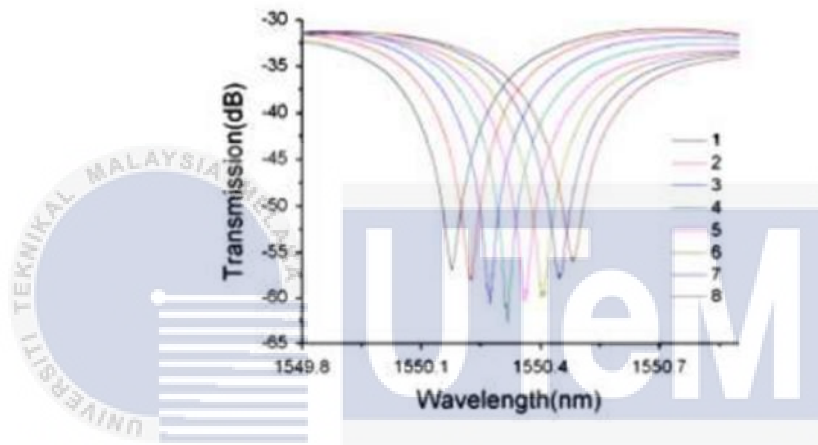
Figure 2.12 Loop and knot resonator resonant wavelength shift as refractometric sensors [18].

Xu et al. developed a refractometric sensor for microfluidic applications that uses a micro-coil resonator with an intrinsic channel [19]. The operation is also similar to a refractometric loop resonator sensor. It is related to the overlapping of the evanescent wave and the analyte during mode propagation in the microfiber. The resonant wavelength shifts when the refractive index changes [19] [20]. The micro coil resonator was coated in Teflon, and the sensor was exposed to isopropanol and methanol. As the refractive index of the analyte increases, the resonant wavelength shifts to a longer wavelength.

The most widely used resonant sensors are heterogeneous sensors that use microfiber to extract light from high-Q resonators such as microcapillaries, microtoroids, microspheres, and microbottle resonators. Coupling efficiencies of up to 90% could be

23

achieved by correctly matching the propagation constant of the mode in the resonator and the microfiber [44]. Because of their large resonator surface, these high-Q resonators are suitable for evanescent sensing for biological and chemical detection. Noto et al. use multiple spheres coated with dextran-biotin hydrogel to detect DNA strands.

2.7   Optical Microfiber Devices

Optical microfiber devices have recently gained popularity, owing to their simplicity of fabrication. This is due to the device's interesting optical properties, which can be used to develop low-cost, miniaturized, all-fiber optical devices for a variety of applications. Many research efforts, have been aimed toward the development of microfiber or nanofiber-based optical resonators that can serve as optical filters, with numerous potential applications in optical communication, laser systems and sensors. Many photonic devices that are typically fabricated as lithographic planar waveguides can also be assembled from microfibers. These microfiber-based devices share functionalities, characteristics, and possibly miniaturization with lithographic planar waveguides. Furthermore, microfiber-based devices could be used as building blocks for larger, more complex photonic circuits in the future. There are three microfiber-based devices are presented, namely MCR, MLR and MKR.

2.7.1   Microfiber Loop Resonator (MLR)

MLRs are made from a single mode microfiber, which is generated by heating and stretching a single mode fiber. Figure 2.13 illustrates a 3mm loop diameter MLR assembled from a 2.0 μm waist diameter microfiber. MLR, like other optical ring resonators, has a 'ring' but is formed of a single mode microfiber. This fabrication can be accomplished with the help of two 3D translation stages, as shown in Figure 2.14. The microfiber is coiled into a

loop by aligning the three-axial position of each translation stage and twisting one of the pigtails. The van der Waals attraction force between two adjacent microfibers is strong enough to withstand the elastic force from the bending microfiber and maintain the microfiber loop structure if the microfiber is sufficiently thin. The loop's diameter can then be reduced by slowly pulling the two SMFs apart using the translation stages. Because of the microfiber's large evanescent field, a coupling region is formed at the close contact of the two microfibers, and a closed optical path is formed within the microfiber loop. Because the MLR is formed of an adiabatically stretched tapered fiber, it has lower connection loss because microfiber-based devices do not experience from the input-output coupling issue that troubles many lithographic planar waveguides. Despite differences in physical structure and fabrication technique, MLR and conventional optical waveguide ring resonators have the same optical characteristics.

Figure 2.13 Image of an MLR taken with an optical microscope

[13].
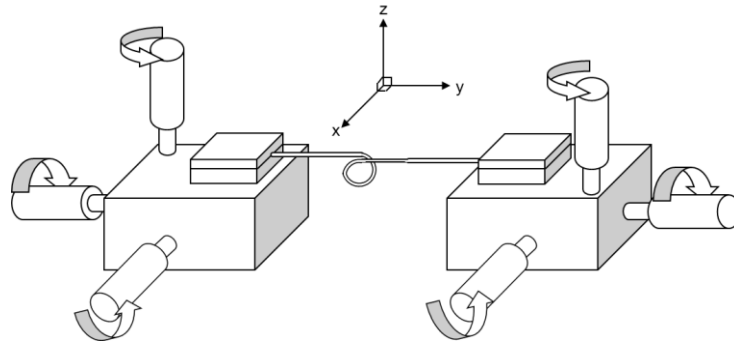
Figure 2.14 MLR manufacturing in two three-dimensional stages **[13]**.

2.7.2   Microfiber Knot Resonator (MKR)

MKR is formed by cutting a long, uniformly tapered fiber into two pieces. One tapered fiber is used to make a microfiber knot, while the other is is used to collect the MKR's output power by connecting the two tapered fiber ends and guiding the output light back to an SMF. Tweezers can be used to make a microfiber knot. In Figure 2.15, the MKR coupling region is denoted by a dashed box, where the two microfibers intertwisted and overlapped in the resonator. Using the flame-brushing method, a 2μm diameter silica microfiber is formed from an SMF. The microfiber is then cut and separated into two unequal parts, one of which is used in the knot fabrication and the other as a collector fiber to collect the transmitted light from the MKR. During the knot's fabrication, a copper wire with a diameter bigger than the diameter of the copper wire is inserted as shown in Figure 2.16 (a). By connecting the two microfiber ends, the light path from the knot resonator is completed. By connecting the two microfiber ends, the light path from the knot resonator is completed. A coupling length of at least 3 mm between two microfibers is required to achieve strong van der Waal attraction force and keep them attached together. The diameter of the microfiber knot is then reduced and fastened to the copper wire by pulling microfibers from both arms of the microfiber knot, as shown in Figure 2.16 (b).

26
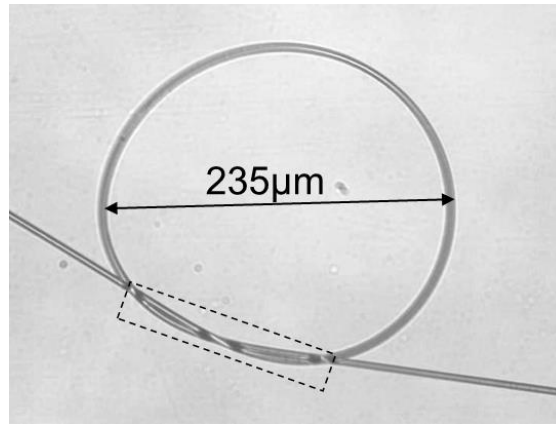
Figure 2.15 Image of an MKR taken with an optical microscope **[13]**.

(a)　　　　　　　　　　　　(b)
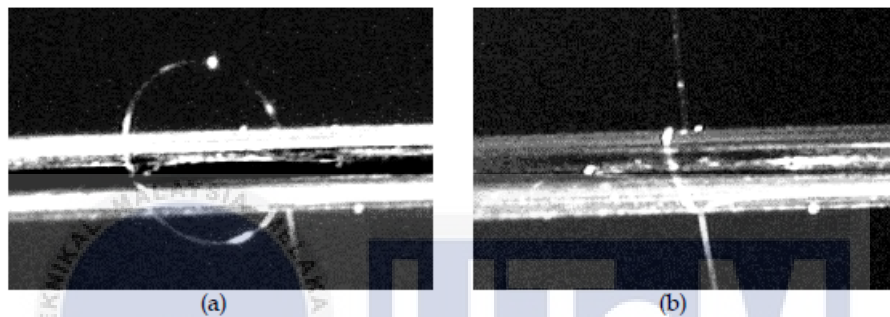
Figure 2.16 MKR optical microscope image tied on a copper wire **[13]**.

2.7.3 Microfiber Coil Resonator (MCR)

Microfiber coil resonators (MCRs) function similarly to other microfiber resonators. It has applications in optical filtering, lasers, and sensors. It can also be used as an optical delay line for an optical communication network due to its small size. It is made by wrapping a long microfiber around a low-index dielectric rod or a rod coated with low-index material. The helical structure of the microfiber coil allows light to propagate along the microfiber, across between the turns of the microfiber in both the forward and backward directions, as shown in Figure 2.17.

27
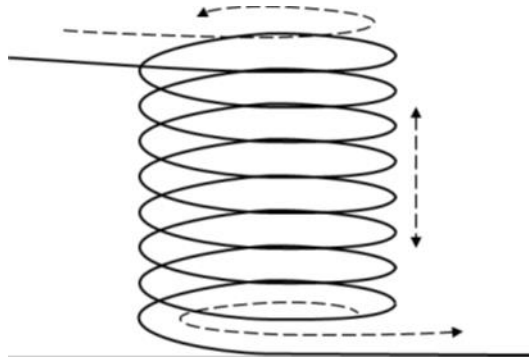
Figure 2.17 Helical structure of an MCR and the direction of light propagation in the resonator **[13]**.

The optical properties of a 1-turn MCR are similar to those of MLR in general. For example, the interference fringes in the MCR transmission spectrum are evenly spaced. When adding more turns to the coil, it is important to ensure they overlap or touch in order to establish coupling between them. With each additional rotation, the MCR's transmission spectrum shifts. Nonetheless, MCR's reproducibility proved tough and problematic. The light propagation properties of MCRs are more sophisticated than those of other microfiber resonators.

2.6   Microfiber Optic's Application

Micro or nano fibers exhibit many unique properties due to their sub-wavelength cross-section, such as tight optical confinement, high fractional evanescent fields, and large manageable waveguide dispersion, which are highly desirable for functionalizing fiber-optic circuits on a micro or nano scale. In the last ten years, the research on Micro or nano has brought numerous opportunities for renewing and expanding fiber optics and technology on the micro or nano scale, as illustrated by the "Micro or nano fibers tree" in Figure 2.18. These recent advances are divided into five categories based on the optics involved including waveguide and near-field optics, nonlinear optics, quantum and atom optics, plasmonics, and optomechanics.

28
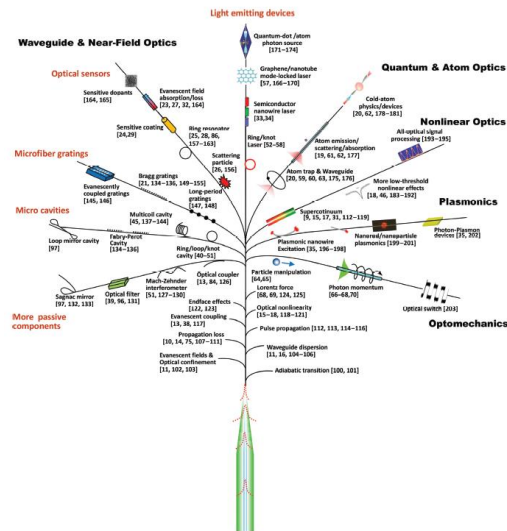
Figure 2.18 A tree plot of common optical Micro or nano fibers applications **[21]**.

2.8 Fiber Optics sensor for CO2 gas detection

Optical fiber gas sensing research started in the 1980s, when it became clear that these sensors could be easily accessed, remotely monitored in real time, and had multiplexing capabilities. Furthermore, because they are non-electrical, they have the potential to operate in hazardous and extreme environments and are intrinsically safe in flammable atmospheres. Colorless, odorless, explosive, asphyxiating, and lighter than air gases can all be detected. This will concentrate on the use of optical fiber as a detector. CO2 detection has recently become a more significant contributor to climate change.

Various sensor configurations to measure CO2 concentrations have been reported over the last two decades. These configurations are classified into three groups based on the mechanism of detection, which fluorescene [22] [23], absorption [24] [25] and refractive index [26] [27]. Fluorescence sensors measure CO2 concentration in solutions based on pH. The dissolution of CO2 in water produces carbonic acid which decreases the pH of the solution. This change in pH can be detected by selected deprotonated dyes coated on the core or tip of an optical fiber. The decrease in pH results in the reduction of fluorescence

intensity at a specific wavelength [23]. Fluorescence sensors for monitoring CO_2 concentration at atmospheric conditions are not suited for downhole applications because of the harsh and high pressure environment that can cause erroneous signals.

The CO_2 concentrations in a gas environment are monitored using absorption-based sensors [24] [25]. There are different kinds of sensor configurations that have been reported which is extrinsic sensors and intrinsic sensors. Extrinsic sensors direct light from a laser source to the gas using an optical fiber. CO_2 has a strong absorption band at 2 μm wavelength, causing the intensity of the transmitted signal to decrease as a function of CO_2 concentration [24]. Intrinsic sensors are based on the interaction of CO_2 and the evanescent field adjacent to an optical fiber. To guide the light in the wavelength range corresponding to CO_2 absorption bands, a multimode fiber is used, and the fiber cladding is removed to extend the evanescent field to the surrounding medium [28] [29]. The transmission signal is a function of CO_2 concentration in the area where the evanescent field of the multimode fiber extends [29]. In addition, microstructured optical fiber can also be used to develop intrinsic sensors. This type of fiber's air holes can be filled with a CO_2-containing gas mixture, resulting in increased interaction between the gas and the light field of the optical modes.

Although absorption based CO_2 sensors can achieve higher resolution in a gas environment, their use to detect liquid CO_2 dissolution in water has not been demonstrated. The main challenge of this is to analyse the complex spectrum absorption bands of multiple fluids present in saline aquifers, such as water, CO_2, CO_2 saturated water, and methane. The CO_2 sensors based on RI have been developed to monitor CO_2 at different pressures. Avdeev et al. studied the use of a fiber tip sensor to distinguish between different CO_2 phases through Fresnel reflection at the interface of the fiber tip [30]. This is a suitable way for monitoring phase changes. However, due to the low RI sensitivity of these devices, using

30

fiber tip sensors to monitor CO2 dissolution in water is difficult. Various sensor configurations have recently been proposed to measure CO2 at atmospheric pressure. Pevec et al. reported the development of a nanowire etched on the tip of an optical fiber [26]. Based on the difference in RI of the two gases, this sensor was able to distinguish between CO2 and H2. Shivananju et al. described a CO2 sensor using carbon nanotubes coated on the core of an etched of FBG [27]. CO2 concentrations as low as 1000 parts per million were measured using this sensor. Despite this, none of these sensor configurations have been shown to be effective in measuring CO2 in deep subsurface environments.

A fiber optic sensor for deep subsurface CO2 monitoring must fulfill a number of performance requirements, including high resolution, mechanical robustness for survival in harsh environments, optical stability to operate over long periods of time and low optical losses to propagate the signal from great depth. In addition, there has been a considerable in research interest on RI-based sensors, allowing for the development of high-resolution sensors capable of continuously monitoring RI [31]. Example of RI sensors include fiber tapers, surface plasmon resonance sensors, grating-based sensors and fiber interferometers. The usual resolution of these devices operating is between 10^{-3} and 10^{-4} RI units [5]. The resolution of grating-based sensors and fiber interferometers can be increased by coating the fiber with a material with a higher RI than the cladding [32]. This method is widely used in long period gratings (LPGs) and, more recently in Mach-Zehnder interferometers (MZIs), that leading to sensor resolutions at the RI of water

2.9   Summary

This chapter will discuss the fabrication techniques for tapered silica microfibers. The theory of light propagation in the tapered optical fibers and methods for their fabrication was discussed briefly. Despite clear advantages, such as high sensitivities and simplicity of

31

fabrication, the wide variety of configurations and their versatility, there are limited reports of practical application of the tapered optical fibers. One of the major challenges for future applications of tapered optical fiber sensors lies in the reliable and reproducible fabrication of the devices. It should be also noted that in simplest form tapered devices are not selectively sensitive and require coating that provide specificity. Thus, three microfiber-based devices also have been reviewed in this chapter which is MLR, MKR and MCR. So far, an optical microfiber has been widely researched in terms of fabrication technique, characteristics, and applications. By reducing optical fiber diameters to the wavelength scale, these tiny fibers have offered a number of favorable properties for manipulating light on the micro or nanoscale, as well as a new platform for both scientific research and technological applications. Based on their capability of waveguiding tightly confined evanescent fields with low losses, strong near field interaction, and miniaturized sizes and several new applications of optical micro or nano in atom optics which may bring new opportunities for utilizing light beyond optics and lead to a great future of fiber optics and technology. In addition, Optical fiber gas sensors are capable of remote sensing and also working in various environments. Evidence is growing that optical fiber gas sensors are superior in a number of ways in some application areas.

CHAPTER 3

METHODOLOGY

3.1   Introduction

This chapter introduces the design process of microfiber optics as a gas sensor which includes detailed information on the tools and components used, the sensor manufacturing process, prototypes and other topics. The proposed study aims to create a microfiber sensor that can detect Carbon dioxide (CO_2) in different concentrations using a tapering method.

3.2   Methodology

This thesis presents a development of an optical microfiber sensor for carbon dioxide in different concentrations using a tapering method. This project focuses on analysing microfiber optic's performance as a gas sensor in detecting carbon dioxide. The selected approach is based on five samples of different concentrations of CO_2 tested, which aims to develop the microfiber optics as a gas sensor to detect CO_2. It consists of several methods, each as applied to various appearances of the whole scope of the methodology. The experimental findings will be described in terms of sensitivity, correlation, and graphical determination coefficients, which depend entirely on the CO_2 concentration and the light source. Subsequently, Figure 3.1 shows the research design of this thesis.
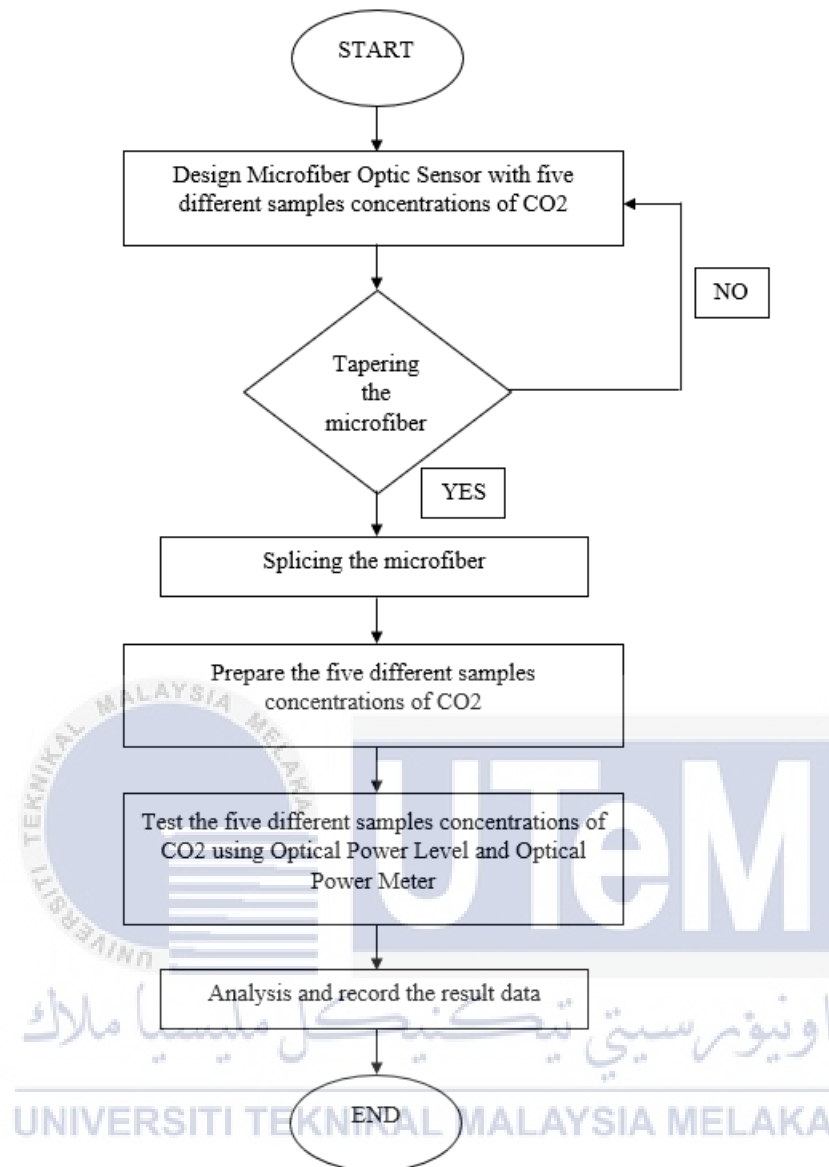
Figure 3.1 Project methodology flowcharts

In order to accomplish project goals, a flowchart was created to guide and summarizes the phases taken steps by steps as shown in figure. 3.1. The project started with the design microfiber optic sensor with five different concentrations of CO2. There are five different samples concentrations of CO2 will be used. The fiber selected for use as the sensor is a single-mode fiber (SMF). The next step is to fabricate tapered fiber is the process of reducing the diameter of the cladding (along with the core) by pulling the fiber's end while heating the fiber's waist. In this case, the smaller diameter taper waists provide higher

34

sensitivity. All microfibers were cut to the same length to reduce losses during the experiment. The mounting part to be stripped for use as a sensor also becomes a strip of the same length. If the splice of the microfiber optic sensors are working, then the process can proceed to the next step; otherwise, it goes to the fiber optic sensor setup.

The next phase was to prepare the five samples of different concentrations of CO_2. An airtight plastic container is used as a medium to trap the CO_2 throughout the experiment. There is a small hole on the top surface of an airtight plastic container. Then, CO_2 gas through respiration is released into the hole of an airtight plastic container by using a straw. The first sample of CO_2 gas was released three times, and it was released about 10% of CO_2 gas then followed by around 20% and 30% and above into the airtight plastic container containing the optical microfiber.

Once the setup is complete, the Optical Power Level will emit a ray to the microfiber, and the result will be taken from the Optical Power Meter. This will determine the reading value due to the different concentrations of CO_2. Following the results, the experiment's findings will be analysed in terms of sensitivity and linearity that are completely dependent on the CO_2 concentration and light source in the form of tables and graphs. In conclusion, the performance of the microfiber optic as a gas sensor is defined as excellent, with sensitivity analysed through transmitted power and wavelength shifting. The linearity of five different concentrations of CO_2 is also defined as good performance.

3.2.1 Tapering Process
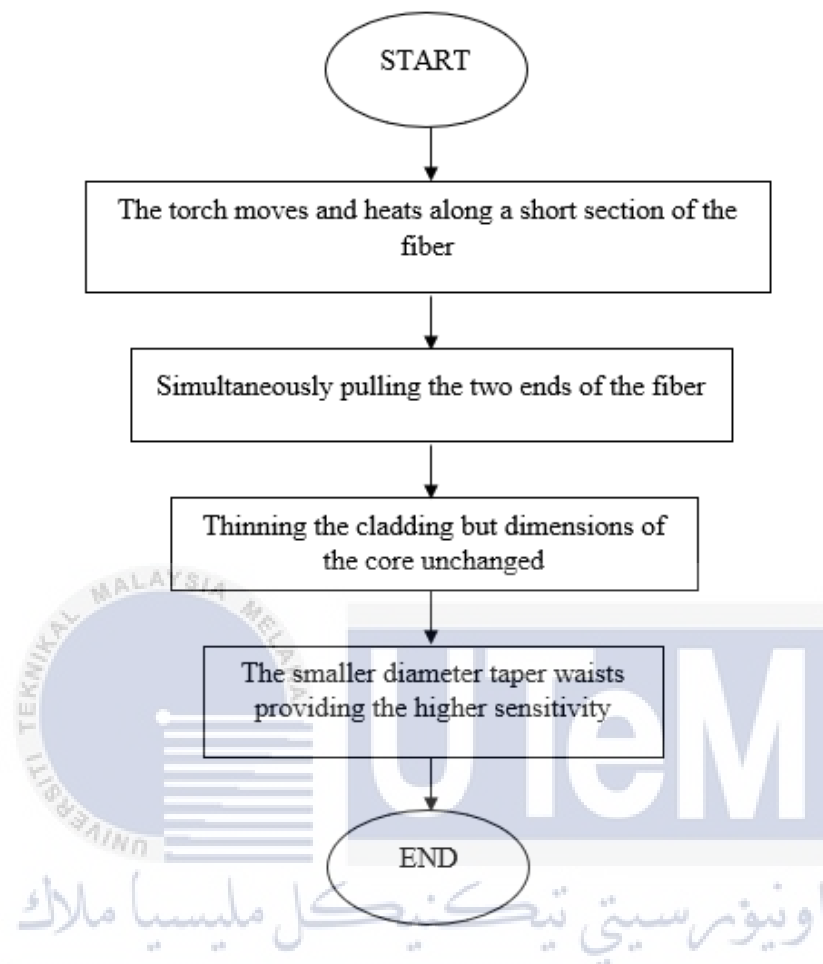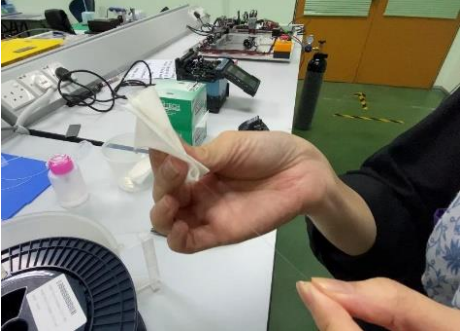
Figure 3.2 Flowchart of the tapering process
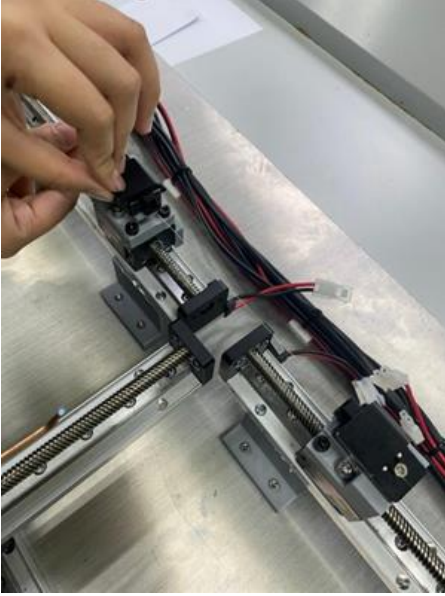
Firstly, a coating length of several cm is removed from the SMF to fabricate tapered microfiber. Next, the SMF is placed horizontally on the translation stage and held by two fiber holders. The torch moves and heats along a short section of the fiber while simultaneously pulling the two ends of the fiber, as shown in Figure 3.2. The heat source comes from a gas burner flame and oxygen. Two stepper motors are incorporated into the rig to control the movement of the torch and translation stage. When a heated glass fiber is stretched, the waist diameter of the fiber is reduced. Along the heat region, the tapered fiber is produced with good uniformity.

In the tapering process, the core and cladding diameters are reduced in the same proportion. The light is coupled from the fundamental mode of the untapered fiber to modes of the tapered section that can interact with the surrounding medium of this process. Other way to facilitate the interaction of light propagating within the optical fiber with the surrounding medium is to thin the cladding of the optical microfiber while leaving the core dimensions unchanged. The tapered microfiber is critical to its sensor performance, with smaller diameter taper waists providing higher sensitivity. The complete procedure on the tapering process is shown in Table 3.1
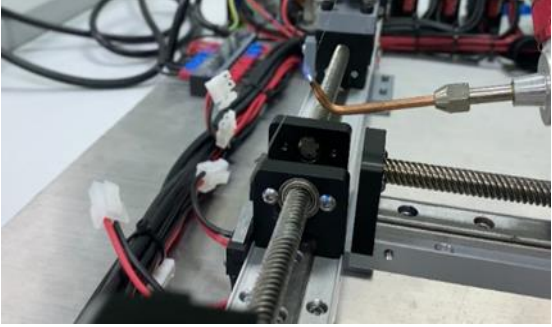
Table 3.1 Complete steps on tapering process
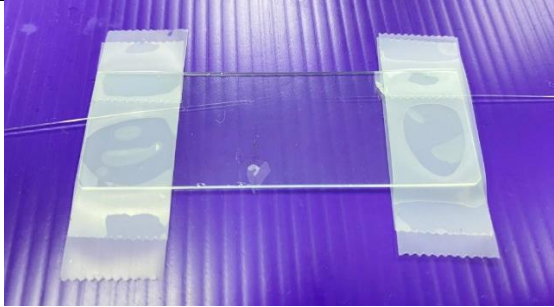
No	Procedure	Description
1		Cut and remove the second layer (cladding) at the centre part of the optical cable using a stripping tool.
2		Remove dust using alcohol and tissues.

3		Place the single-mode fiber horizontally on a translation stage held by two fiber holders.
4		Set a perfect small flame and controlled the flame movement.
5		The torch moves and heats along a short section of the fiber while simultaneously pulling the two ends of the fiber.

6		In the tapering process, when heated glass fiber is stretched, the waist diameter of the fiber is reduced.
6		Control the movement of the torch backwards and extinguish the flame.
7		Tapered optical microfiber.
8		On the translation stage, open the holders with care.

9		Place a tapered microfiber on microscope slides.

3.2.2 Splicing Process
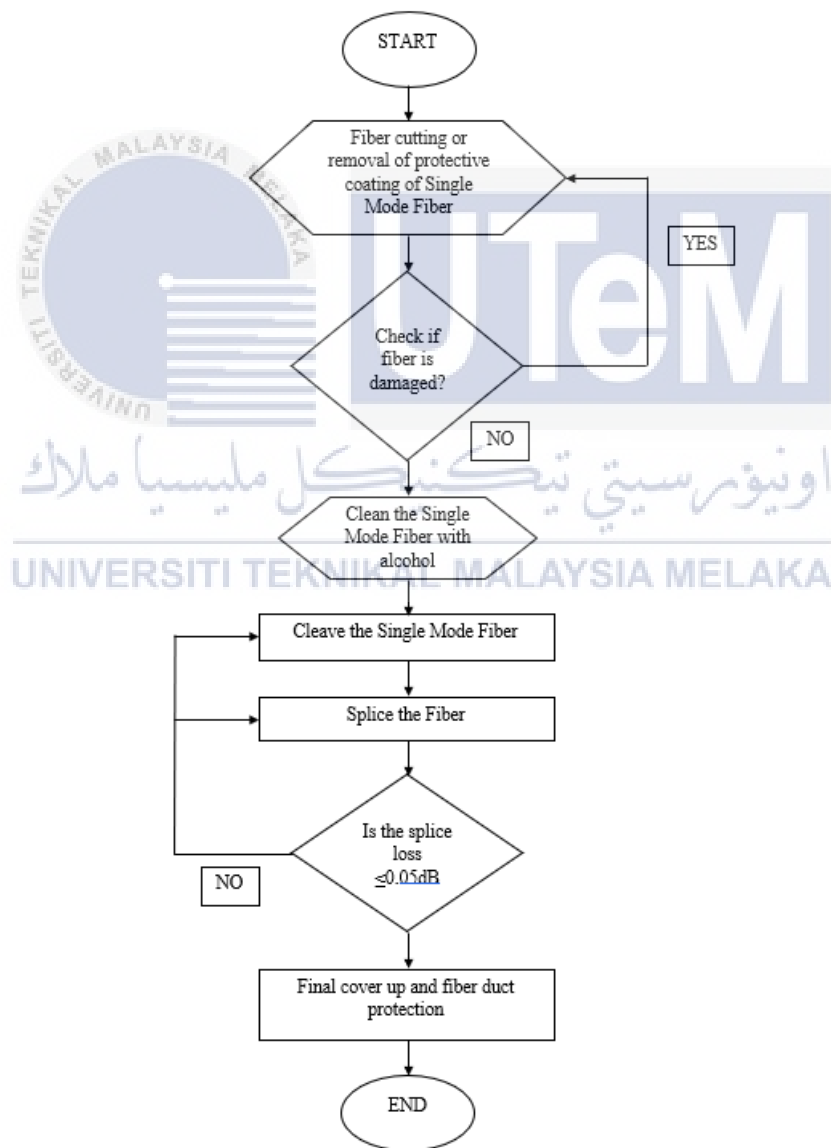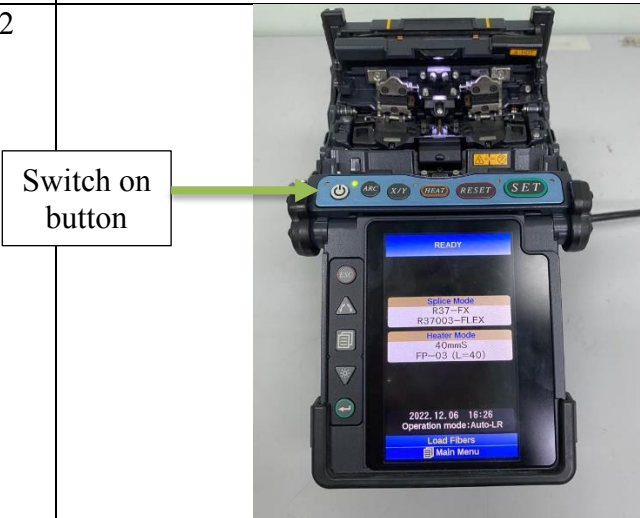
Figure 3.3 Flowchart of splicing process
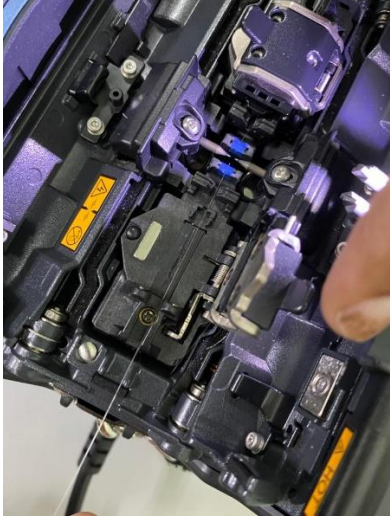
First, a fiber optic cable stripper is used to remove the Single-Mode Fiber layer. Afterwards, the fibers are cleaned with alcohol to remove coating residues or dust. Next, the fibers are cleave using a high precision cleaver Fujikura CT-30 cutter to achieve a 90°-degree angle. The Fujikura FSM-18R splicing tool is used to join two fibers that have been stripped from their lining and cleaned. The fibers will be placed on top of the separator, with the fibers aligned in the same location. The complete procedure on how to connect is shown in Table 3.2.

Table 3.2 Complete steps for Splicing using Fujikura FSM-18R

No	Procedure	Description
1		List of the apparatus used in splicing.
2		Press the 'ON' button to turn on the Fujikura FSM-18R.

3		Cut the outer layer of the optical cable.
4		Remove the second layer (cladding) on the optical cable.
5		Remove dust using alcohol and tissues.
6		Cleave the optical cable using high-precision cleaver Fujikura CT-30 cutter to achieve a 90°-degree angle.

7		Place the cable on the separator, and make sure the cable is in the same position.
8	'SET' button	Press on 'SET' button and wait until the connection is complete.

9		The connecting cable is ready to be laid on impra board.

3.2.3 Experimental Setup Process

This section will proceed with the process from the beginning until the end of the procedure to achieve the purpose of this project.

3.2.3.1 Preparations of Tapered Microfiber Sensor

For the process preparations of tapered silica microfiber can see in Table 3.1 and these are five samples of tapered microfiber fabrication based on tapering method as shown in Figure 3.4.

44
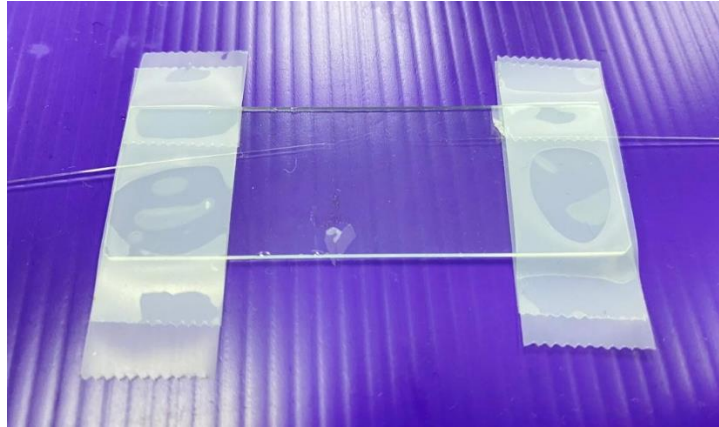
Figure 3.4 Tapered silica microfiber

3.2.3.2 Plastiscine

The function of the plasticine surrounding the tapered microfiber area is the medium used to compress an airtight container so that no air can get in or out immediately after CO_2 gas is released as shown in Figure 3.5.

Figure 3.5 Plasticine

3.2.3.3 An airtight container used to trap CO2 gas

The functionality of an airtight plastic container is used as a medium to trap the CO_2 throughout the experiment. There is a small hole on the top surface of an airtight plastic container. Then, CO_2 gas through respiration is released into the hole of an airtight plastic

45

container using a straw, as shown in Figure 3.6. The first sample of CO_2 gas was released

three times, and it was released about 10% of CO_2 gas then, followed by around 20% and

30% and above, into the airtight container containing the optical microfiber. This will

determine the reading value of sensitivity and linearity of different concentrations of CO_2

that have been released.
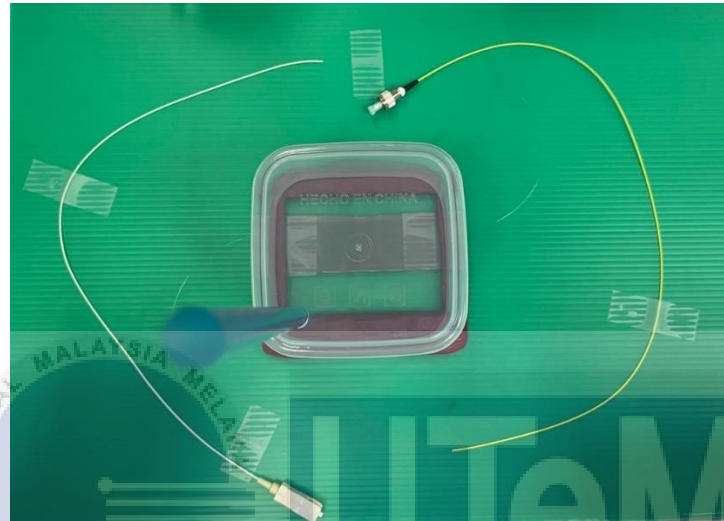
Figure 3.6 An airtight container containing tapered microfiber in different concentrations of CO_2

3.2.3.4 Procedure material and equipment setup

Firstly, prepare the Optical Power Level and Optical Power Meter by setting the

wavelength to 1550nm and plugging the microfiber optic pigtail as illustrated in Figure 3.7.

Then, as shown in Figure 3.8, an airtight plastic container containing the tapered microfiber

sensor in different concentrations of CO_2 will be tested. Next, the 1550nm or 1310nm light

source from the Optical Power Level will emit different concentrations of CO_2. Finally, for

each different concentration of CO_2, it can be monitored by the Optical Power Meter, with

the output measured in decibels (dBm) and taken at two wavelengths, 1550nm and 1310nm.

Following the results, the experiment's findings will be analysed in terms of sensitivity and

46

linearity, which are completely dependent on the CO_2 concentration and light source in the form of tables and graphs.

Figure 3.7 Optical power level and optical power meter

Figure 3.8 Tapered microfiber sensor in different concentrations of CO_2.

3.3   Tools and materials

All materials and equipment used in the project are shown in Table 3.3
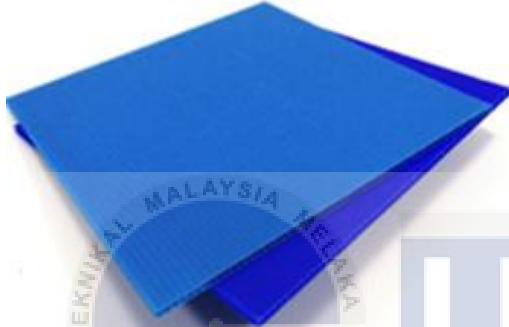
Table 3.3 Equipment and material used in the project

No	Material and Equipment	Description
1	SimpliFiber® Optical Power Level	- Source of input that is connected to the microfiber. - The wavelength is set at 1550nm and 1310nm.
2	Mini-OTDR Optical Power Meter	- The output is measured and sent to the display. - The device that displays the result is the output device.
3	Commercial Splicer Fujikura FSM-18R	- Splice the microfibers together.

4	High Precision Cleaver Fujikura CT-30	- Obtain the flat tip of the microfiber at 90°-degree angle.
5	Microfiber Optic Stripper	- Remove the cladding on the optical microfiber.
6	Single Mode Fiber	- Used in sensor development. - The size of fiber optic is 125nm.

7	Single Mode Connector	-	Use to connect an optical spectrum analyser to a sensor.
8	Rubbing Alcohol	-	Remove the residual or dust after cleaving and before splicing.
9	Tissue	-	Use together with alcohol to clean the fiber.

10	Microscope Slides	- The medium used to lay the tapered microfiber.
12	Tape Dispenser	- Used to secure the tapered microfiber on the microscope slides.
11	Airtight Plastic Container	- CO2 gas is released into the airtight container containing optical microfiber.

11	Plasticine	- The medium that is used to compress an airtight container so that no air can get in or out immediately after CO_2 gas is released.
12	Impra board 27'' x 30''	- To place the fiber after the fiber been splice. - Used as the main supply point for experiments.

3.4 Experimental setup of the project

In this section, the setup of the optical microfiber sensor will show the flow of connecting components and equipment with their functions along with the methods used.

3.4.1 Tapered microfiber using a tapering method

Firstly, a coating length of several cm is removed from the SMF to fabricate tapered fiber. Then, the SMF is placed horizontally on the translation stage and held by two fiber holders. Next, during the tapering process, the torch moves and heats along a short section of the fiber while simultaneously pulling the two ends of the fiber, as shown in Figure 3.9. The heat source comes from a gas burner flame and the oxygen. An oxy-butane torch flame

52

width diameter is 1mm. Two stepper motors are incorporated into the rig to control the movement of the torch and translation stage. When a heated glass fiber is stretched, the waist diameter of the fiber is reduced. As a result, the tapered fiber is produced along the heat region with good uniformity.
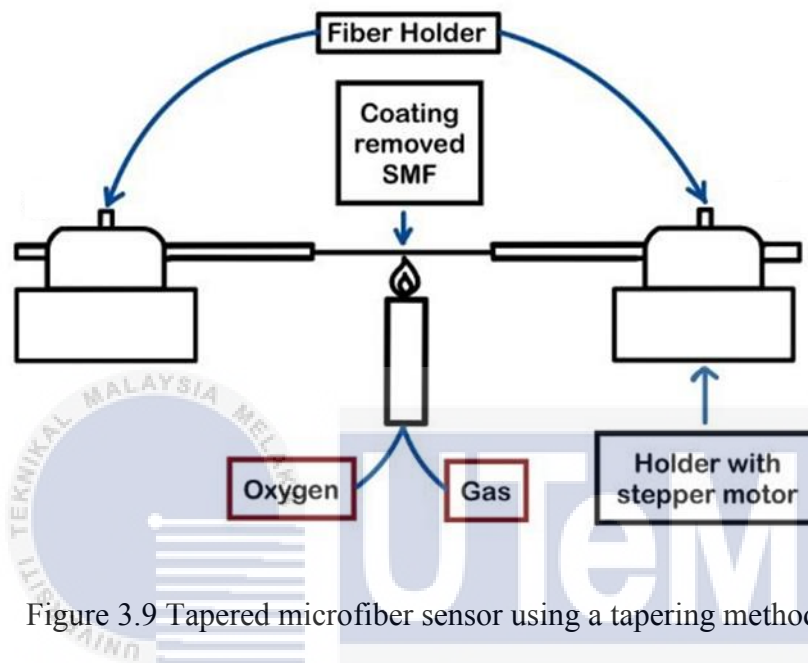
Figure 3.9 Tapered microfiber sensor using a tapering method

3.4.2 Microfiber optics sensor to detect CO2 gas

To evaluate the different concentrations in CO_2, tapered microfiber optic sensors are connected to an Optical Power Level as an input. The Optical Power Level emits a wavelength of 1550nm or 1310nm to the fiber. The result is then recorded in dBm by the Optical Power Meter, as shown in Figure 3.10 below.
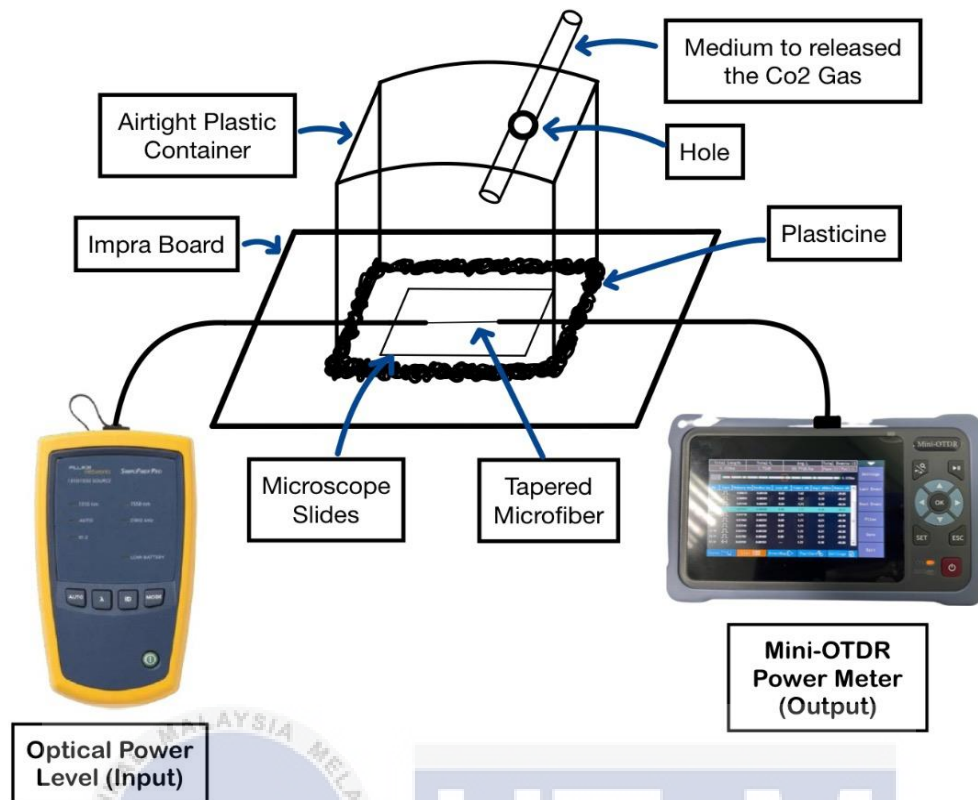
Figure 3.10 Model of project

There will be five samples of different concentrations of CO_2 will be tested. The optical microfiber will act as a sensor to detect the CO_2 in different concentrations. The CO_2 gas is released three times for the first sample. It released about 10% CO_2 gas then, followed by around 20% and 30% and above, into the airtight plastic container containing the optical microfiber. This will determine the reading value due to the different concentrations of CO_2.

Following the results, the experiment's findings will be described in terms of sensitivity, correlation and coefficient of determination of the graph, which are all completely dependent on the CO_2 concentration and different light sources.

3.5   Limitation of the proposed methodology

One of the limitations observed in this project is the challenges in fabricating reliable and reproducible devices for applications involving tapered microfiber optic sensors. It should also be noted that in simplest form tapered devices are not selectively sensitive and require specificity coating. Furthermore, including technical issues pertaining to the complicated handling of microfiber during the process and maintaining their performance at a reasonable cost. Next, the equipment used is insufficient and limited, where students have to use the Ftkmp building's laboratory.

3.6   Summary

The proposed methodology for developing an optical microfiber sensor for carbon dioxide in different concentrations using a tapering method is presented in this chapter. The proposed methodology's main goal is to achieve an excellent outcome in order to obtain a superior waveform output value from the Optical Power Level and Optical Power Meter. The main purpose of the technique used is to maximise efficiency, ease of use and manipulation, and the practicality of microfiber optic sensors rather than achieve the maximum accuracy level.

CHAPTER 4

RESULTS AND DISCUSSIONS

4.1 Introduction

This chapter presents the results and analysis of the development of an optical microfiber sensor for carbon dioxide in different concentrations using a tapering method. A case study was conducted to demonstrate the optical microfiber sensor's sensitivity. The performance of microfiber optics as a gas sensor in detecting CO_2 is used in the case study to determine the sensitivity of CO_2 in different concentrations. This will determine the reading value due to the different CO_2 concentrations. Following the results, the experimental findings will be described in terms of sensitivity, correlation and coefficient of determination of the graph, which completely depends on the CO_2 concentrations and light sources.

4.2 Results and Analysis

The following table shows the analysis of microfiber optics as a gas sensor to detect CO_2 in different concentrations. These analyses are divided into several pieces of information, including measurements of the diameter and thickness of optical microfibers, the percentage of CO_2 gas released, the time took every few minutes based on the percentage of gas released, sensitivity and percentage of linearity in different CO_2 concentrations. Based on the data and analysis, the higher the linearity value, the higher the sensitivity towards the sensor.

4.2.1 Size diameter of microfiber optics after tapering process

After tapering, we borrowed a Measuring Microscope (Nikon Industrial Metrology) from the FTKMP laboratory to measure the diameter of the tapered microfiber optics. Initially, the fiber diameter size was 225µm. The figure below shows the microfiber at a diameter of 58.0µm after the tapering process.
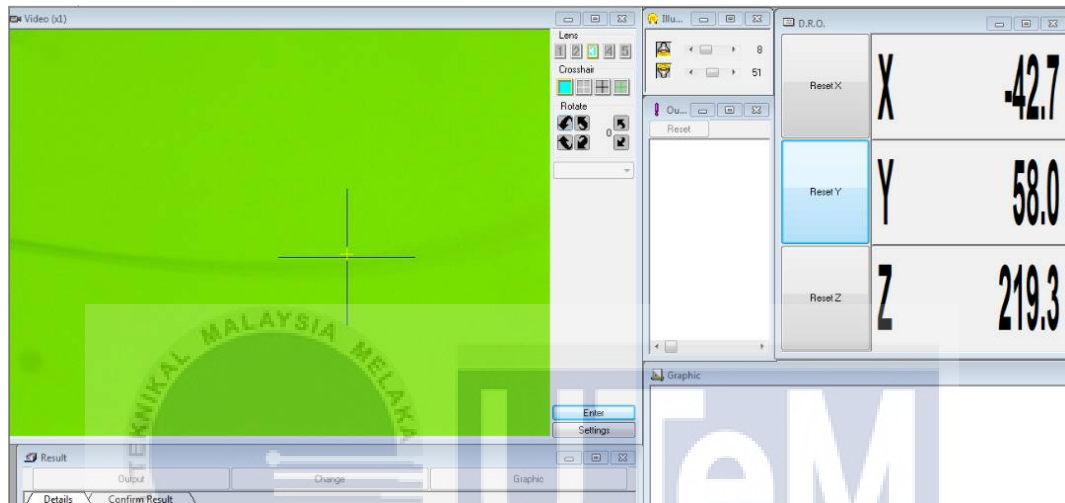
Figure 4.1 Microscopic image of microfiber size diameter after the tapering process

4.2.2 Sensitivity of microfiber optics sensor on 10% CO2 gas released

The analysis is based on the sensitivity and linearity percentage of the performance on microfiber optics as a gas sensor in different CO_2 concentrations that were carried out during the test. Through this analysis, the output power have been observed and recorded for every concentration using different wavelengths as shown in Table 4.1. The first release was about 10% of CO_2 gas, followed by around 20% and 30% and above.

Table 4.1 Comparison of data collected for the experiment

Time (minutes)	10% CO2 gas released	
	At wavelength 1550nm	At wavelength 1310nm
1	-37.01	-41.84
2	-37.19	-41.84
3	-37.21	-42.25
4	-37.21	-42.31
5	-37.21	-42.31
6	-37.21	-42.31
7	-37.21	-42.31
8	-37.21	-42.31
9	-37.21	-42.31

Table 4.2 Sensitivity and Linearity of 10% CO2 gas released

	10% CO2 gas released at wavelength 1550nm	10% CO2 gas released at wavelength 1310nm
Sensitivity (dBm)	-0.0143	-0.0568
Linearity %	59.33	76.14

At the percentage of 10% CO2 gas released showed a higher sensitivity value at wavelength 1310nm rather than at 1550nm wavelength, where it manages to have -0.0568dBm based on table 4.2. This cycle continued three times for every concentration, which helped to reduce random error during data observation. Linearity at a percentage of 10% CO2 gas released is then calculated:-

$$\text{Linearity} = (\sqrt{R^2}) \times 100.$$

In comparison, at the wavelength between 1550nm and 1310nm, we can clearly see that at the wavelength of 1310nm has the greatest linearity that is resulting the data to fit in the linear graph. This shows that the highest value will perform microfiber optics better as a gas sensor. At wavelength 1310nm, has strong linear relationship compared to the wavelength of 1550nm, with the linearity 76.14% of the 10% gas released interacting with

the light source passing through it, and the sensitivity value for 1310nm is higher than

1550nm wavelength.

Figure 4.2 Sensitivity of microfiber optics sensor on 10% gas released

Based on Figure 4.2, shows two different lines for sensitivity with the total outcome

percentage of 30% CO2 gas released at 1550nm and 1310nm wavelengths. Each experiment

was checked every 1 minute for a total of 9 minutes at wavelength 1550nm and 1310nm,

with the output measured in decibels (dBm). The optical microfiber acts as a sensor to detect

the CO2 gas and perform in different concentrations using different wavelengths. Sensitivity

and linearity were used as observed parameters. There is a distinct tendency where the cycle

will go up and down before returning to its initial value. According to the investigation,

based on the parameters, at a wavelength of 1310nm, it will show that the optical microfiber

sensor has better performance. There is strong positive linear correlation between time and

59

power (dBm). As the time increase, the power also increase. This experiment also determines that the microfiber optics as a gas sensor is used to sense the sensitivity.

4.2.3 Sensitivity of microfiber optics sensor on 20% gas released

The second analysis is based on the sensitivity and linearity percentage of the performance on microfiber optics as a gas sensor in different CO2 concentrations that were carried out during the test. Through this analysis, the output power have been observed and recorded for every concentration using a different wavelength, as shown in Table 4.3. The first release was about 10% CO2 gas then, followed by around 20% and 30% and above.

Table 4.3 Comparison of data collected for the experiment

Time (minutes)	20% CO2 gas released	
	At wavelength 1550nm	At wavelength 1310nm
1	-36.57	-40.48
2	-36.85	-40.48
3	-36.88	-41.07
4	-36.88	-41.09
5	-36.88	-41.1
6	-36.88	-41.1
7	-36.88	-41.1
8	-36.88	-41.1
9	-36.88	-41.1

Table 4.4 Sensitivity and Linearity of 20% CO2 gas released

	20% CO2 gas released at wavelength 1550nm	20% CO2 gas released at wavelength 1310nm
Sensitivity (dBm)	-0.0222	-0.0735
Linearity %	59.19	74.26

At the percentage of 20% CO2 gas released showed higher sensitivity value at wavelength 1310nm rather than at 1550nm wavelength, where it manages to have -

0.0735dBm based on table 4.4. This cycle continued three times for every concentration, which helped to reduce random error during data observation. Linearity at a percentage of 20% CO2 gas released is then calculated:-

$$\text{Linearity} = (\sqrt{R^2}) \times 100.$$

In comparison, at the wavelength between 1550nm and 1310nm, we can clearly see that the wavelength of 1310nm has the greatest linearity, resulting in the data fitting in the linear graph. This shows that the highest value will perform microfiber optics better as a gas sensor. At wavelength 1550nm, it almost have a perfect correlation compared to the wavelength of 1310nm, with the linearity 74.26% of the 20% gas released interacting with the light source passing through it, and the sensitivity value is higher than 1550nm wavelength.
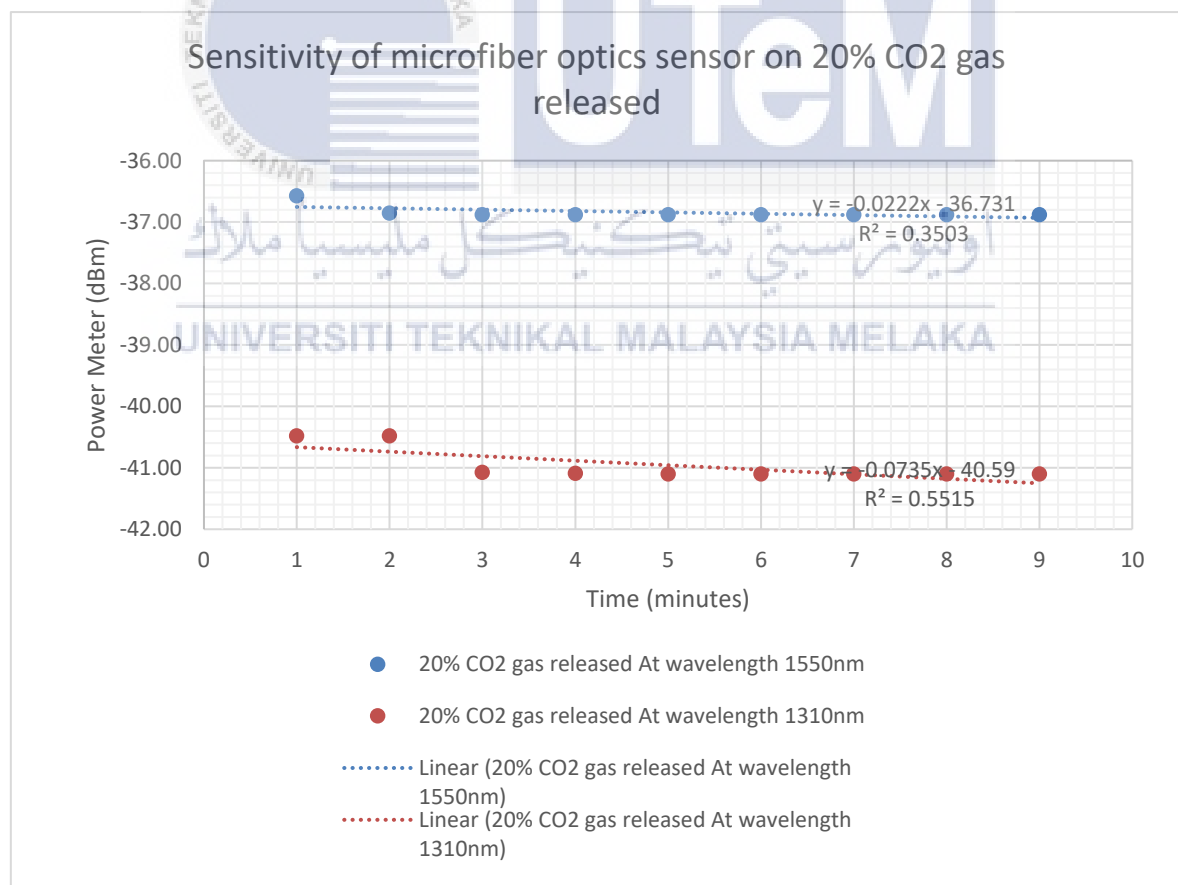
Figure 4.3 Sensitivity of microfiber optics sensor on 20% CO2 gas released

Based on Figure 4.3, shows two different lines for sensitivity with the total outcome percentage of 30% CO2 gas released at 1550nm and 1310nm wavelengths. Each experiment has been checked every 1 minute for a total of 9 minutes at wavelengths 1550nm and 1310nm, with the output measured in decibels (dBm). The optical microfiber act as a sensor to detect the CO2 gas and perform in different concentrations by using different wavelengths. Sensitivity and linearity were used as observed parameters. There is a distinct tendency where the cycle will go up and down before returning to its initial value. According to the investigation, based on the parameters, at a wavelength of 1310nm, it will show that the optical microfiber sensor has better performance. There is strong positive linear correlation between time and power (dBm). As the time increase, the power also increase. This experiment also determines that the microfiber optics as a gas sensor used to sense the sensitivity.

4.2.4   Sensitivity of microfiber optics sensor on 30% CO2 gas released

The third analysis was also based on the sensitivity and linearity percentage of the performance on microfiber optics as a gas sensor in different CO2 concentrations that were carried out during the test. Through these analysis the output power have been observed and recorded for every concentration by using a different ofis analysis, the output power have been observed and recorded for every concentration using a different wavelength, as shown in Table 4.5. For the first released was about 10% of CO2 gas then following around 20% and 30% and above.

Table 4.5 Comparison of data collected for the experiment

Time (minutes)	30% CO2 gas released	
	At wavelength 1550nm	At wavelength 1310nm
1	-38.29	-44.47
2	-39.5	-44.73
3	-40.14	-45.15
4	-40.24	-45.18
5	-40.29	-45.19
6	-40.32	-45.17
7	-40.32	-45.17
8	-40.32	-45.17
9	-40.32	-45.18

Table 4.6 Sensitivity and Linearity of 30% CO2 gas released

	30% CO2 gas released at wavelength 1550nm	30% CO2 gas released at wavelength 1310nm
Sensitivity (dBm)	-0.1837	-0.0698
Linearity %	73.58	73.26

At the percentage of 30% CO2 gas released showed higher sensitivity value at wavelength 1550nm rather than at 1310nm wavelength, where it manages to have -0.1837dBm based on table 4.6. This cycle continued three times for every concentration, which helps to reduce random error during data observation. Linearity at a percentage of 30% CO2 gas released is then calculated:-

$$\text{Linearity} = (\sqrt{R^2}) \times 100.$$

In comparison, at the wavelength between 1550nm and 1310nm, we can clearly see that both wavelengths have strong linearity that resulting the data to fit in the linear graph. This shows that the highest value would give a better performance of microfiber optics as a gas sensor. At wavelength 1310nm, it almost have the highest correlation compared to the wavelength of 1550nm, with the linearity of 73.58% of the 30% gas released interacting with

63

the light source passing through it, and the sensitivity value for 1550nm is higher than
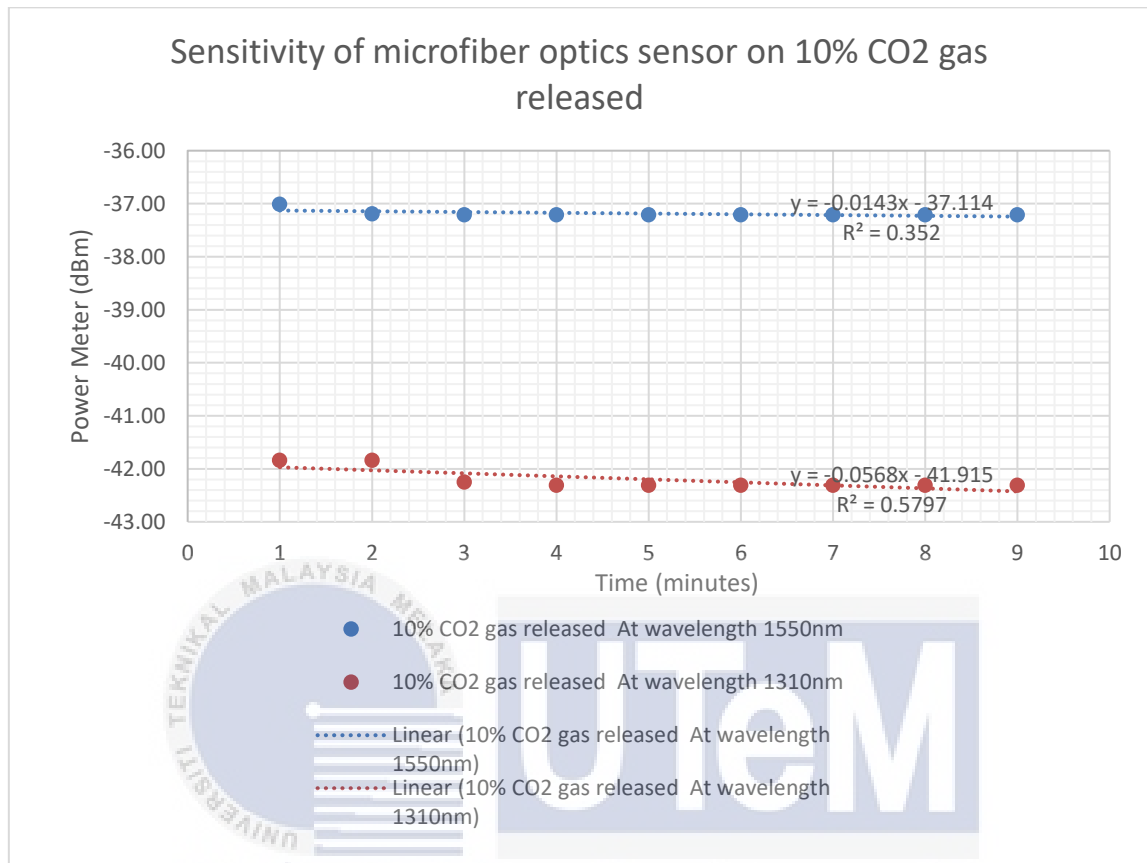
1310nm wavelength.

Figure 4.4 Sensitivity of microfiber optics sensor on 30% CO2 gas released

Based on Figure 4.4, shows two different lines for sensitivity with the total outcome

percentage of 30% CO2 gas released at 1550nm and 1310nm wavelengths. Each experiment

has been checked every 1 minute for a total of 9 minutes at wavelengths 1550nm and

1310nm, with the output measured in decibels (dBm). The optical microfiber acts as a sensor

to detect the CO2 gas and perform in different concentrations using different wavelengths.

Sensitivity and linearity were used as observed parameters. There is a distinct tendency

where the cycle will go up and down before returning to its initial value. According to the

investigation, based on the parameters, at a wavelength of 1550nm, it will show that the

optical microfiber sensor has better performance. There is strong positive linear correlation

between time and power (dBm). As the time increase, the power also increase. This experiment also determines that the microfiber optics as a gas sensor used to sense the sensitivity.

4.2.5   Sensitivity of microfiber optics sensor on 40% gas released

Fourth analysis was also based on the sensitivity and linearity percentage of the performance on microfiber optics as a gas sensor in different CO_2 concentrations that were carried out during the test. Through this analysis, the output power have been observed and recorded for every concentration using a different wavelength, as shown in Table 4.7.

Table 4.7 Comparison of data collected for the experiment

Time (minutes)	40% CO_2 gas released	
	At wavelength 1550nm	At wavelength 1310nm
1	-36.53	-44.48
2	-36.53	-44.59
3	-36.71	-45
4	-36.75	-45.11
5	-36.75	-45.12
6	-36.75	-45.11
7	-36.75	-45.11
8	-36.75	-45.11
9	-36.75	-45.11

Table 4.8 Sensitivity and Linearity of 40% CO_2 gas released

	40% CO_2 gas released at wavelength 1550nm	40% CO_2 gas released at wavelength 1310nm
Sensitivity (dBm)	-0.027	-0.0717
Linearity %	77.51	78.05

At the percentage of 40% CO_2 gas released showed higher sensitivity value at wavelength 1310nm rather than at 1550nm wavelength, where it manages to have -

0.0717dBm based on table 4.8. This cycle continued three times for every concentration, which helps to reduce random error during data observation. Linearity at a percentage of 40% CO2 gas released is then calculated:-

$$Linearity = (\sqrt{R^2}) \times 100.$$

In comparison, at the wavelength between 1550nm and 1310nm, we can clearly see that the wavelength of 1310nm has the greatest linearity, resulting in the the data fitting in the linear graph. This shows that the highest value will perform microfiber optics better as a gas sensor. At wavelength 1550nm, it almost have a strong linear relationship compared to the wavelength of 1310nm, with the linearity 78.05% of the 40% gas released interacting with the light source passing through it, and the sensitivity value is higher than 1550nm wavelength.
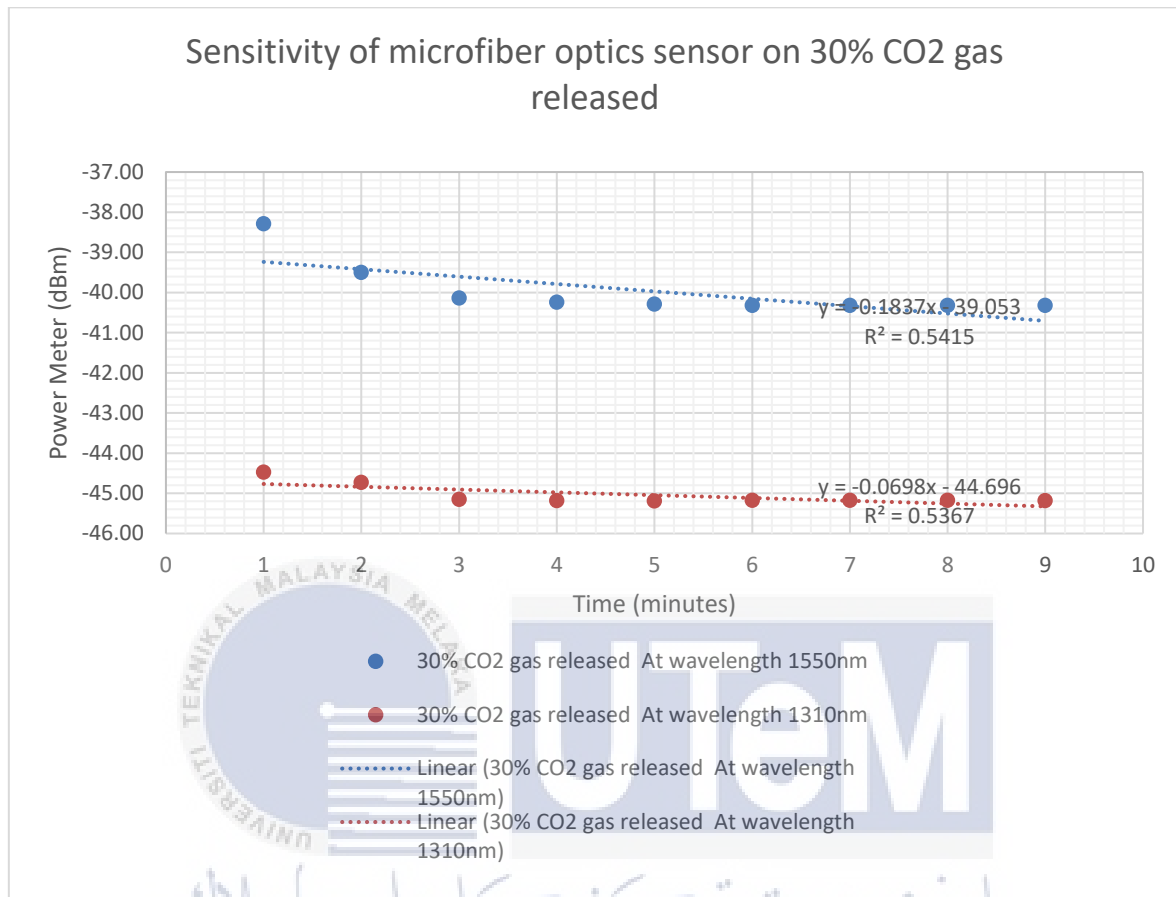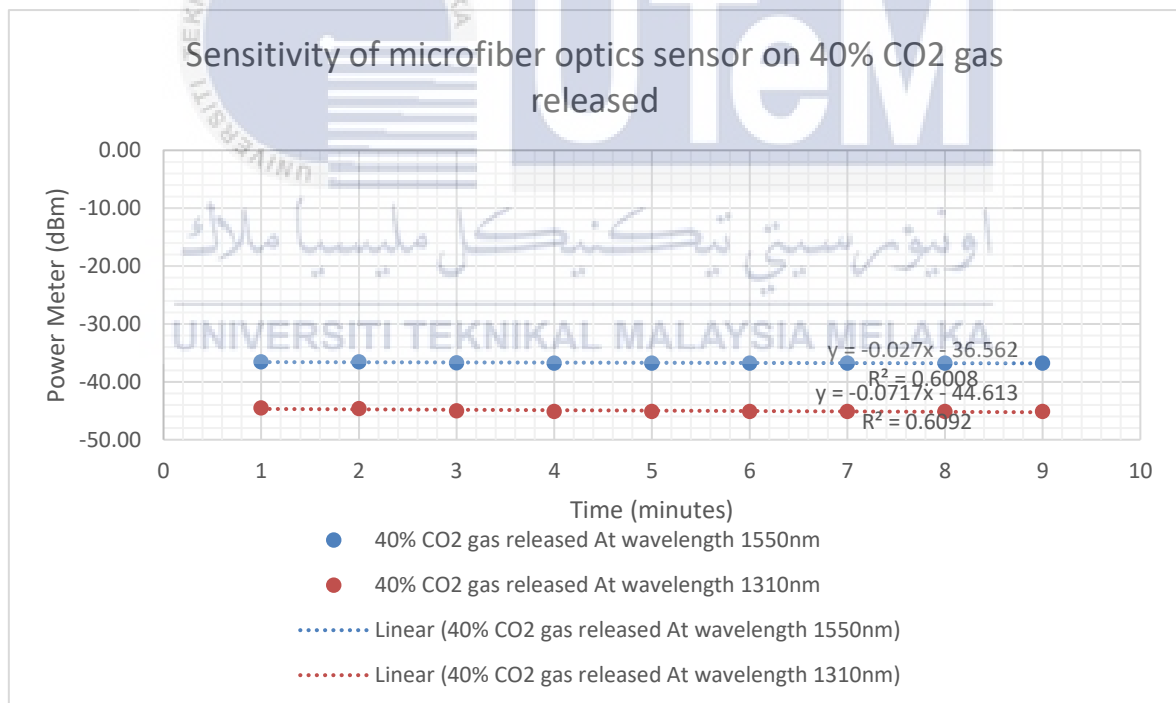

Figure 4.5 Sensitivity on microfiber optics sensor on 40% gas released

Based on Figure 4.5, shows two different lines for sensitivity with the total outcome percentage of 40% CO2 gas released at 1550nm and 1310nm wavelengths. Each experiment has been checked every 1 minute for a total of 9 minutes at wavelengths 1550nm and

1310nm, with the output measured in decibels (dBm). The optical microfiber acts as a sensor to detect the CO2 gas and perform in different concentrations using different wavelengths. Sensitivity and linearity were used as observed parameters. There is a distinct tendency where the cycle will go up and down before returning to its initial value. According to the investigation, based on the parameters, at a wavelength of 1310nm, it will show that the optical microfiber sensor has better performance. There is strong positive linear correlation between time and power (dBm). As the time increase, the power also increase. This experiment also determines that the microfiber optics as a gas sensor used to sense the sensitivity.

4.2.6 Sensitivity on microfiber optics sensor on 50% gas released

The last analysis is based on the sensitivity and linearity percentage of the performance on microfiber optics as a gas sensor in different CO2 concentrations that were carried out during the test. Through this analysis, the output power have been observed and recorded for every concentration using a different wavelength, as shown in Table 4.9. The first release was about 10% CO2 gas then, followed by around 20% and 30% and above.

Table 4.9 Comparison of data collected for the experiment

Time (minutes)	50% CO2 gas released	
	At wavelength 1550nm	At wavelength 1310nm
1	-41.84	-40.53
2	-41.84	-40.61
3	-42.25	-40.76
4	-42.31	-40.76
5	-42.31	-40.76
6	-42.31	-40.76
7	-42.31	-40.75
8	-42.31	-40.76
9	-42.31	-40.76

Table 4.10 Sensitivity and Linearity of 40% CO2 gas released

	CO2 gas released about 50% at wavelength 1550nm	CO2 gas released about 50% at wavelength 1310nm
Sensitivity (dBm)	-0.0568	-0.0225
Linearity %	76.14	72

At the percentage of 50% CO2 gas released showed higher sensitivity value at wavelength 1550nm rather than at 1310nm wavelength, where it manages to have -0.0568dB based on table 4.10. This cycle continued three times for every concentration, which helped to reduce random error during data observation. Linearity at a percentage of 50% CO2 gas released is then calculated:-

$$\text{Linearity} = (\sqrt{R^2}) \times 100.$$

In comparison, at the wavelength between 1550nm and 1310nm, we can clearly see that the wavelength of 1550nm has the greatest linearity, resulting in the data fitting in the linear graph. This shows that the highest value will perform microfiber optics better as a gas sensor. At wavelength 1310nm, it almost have a strong linear relationship compared to the wavelength of 1550nm, with the linearity 76.14% of the 50% gas released interacting with the light source passing through it, and the sensitivity value is higher than 1310nm wavelength.
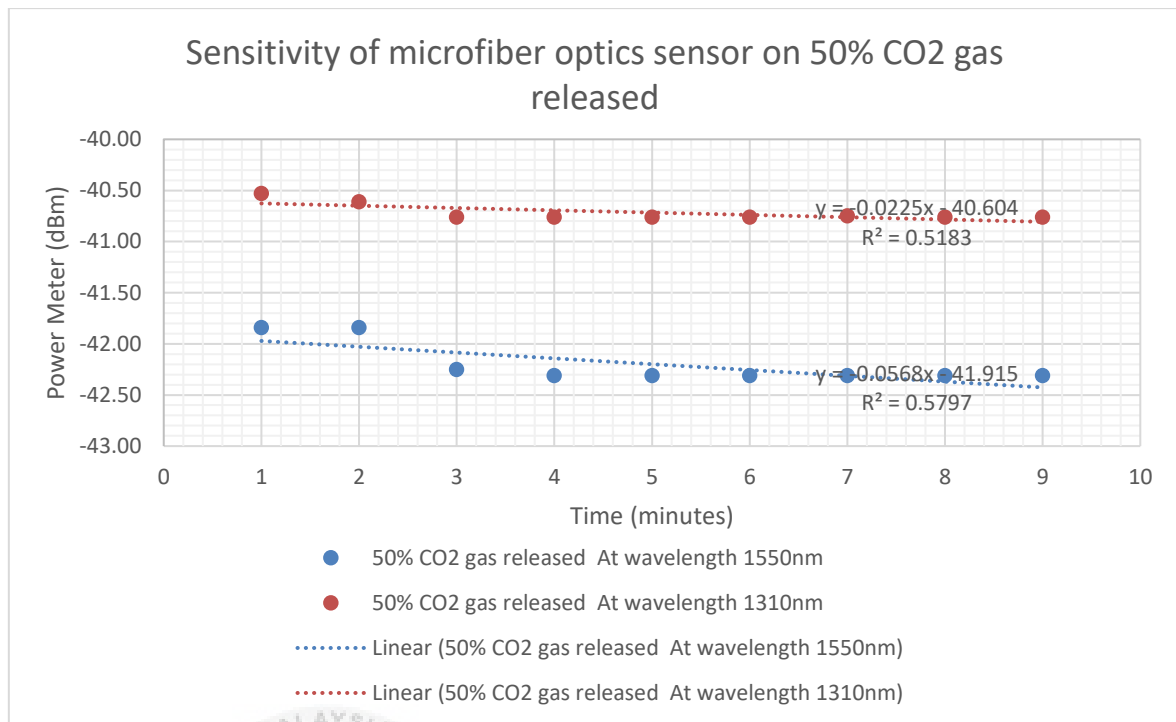
Figure 4.6 Sensitivity on microfiber optics on 50% gas released

Based on Figure 4.6, shows two different lines for sensitivity with the total outcome percentage of 50% CO2 gas released at 1550nm and 1310nm wavelengths. Each experiment has been checked every 1 minute for a total of 9 minutes at wavelengths 1550nm and 1310nm, with the output measured in decibels (dBm). The optical microfiber acts as a sensor to detect the CO2 gas and perform in different concentrations using different wavelengths. Sensitivity and linearity were used as observed parameters. There is a distinct tendency where the cycle will go up and down before returning to its initial value. According to the investigation, based on the parameters, at a wavelength of 1550nm, it will show that the optical microfiber sensor has better performance. There is strong positive linear correlation between time and power (dBm). As the time increase, the power also increase. This experiment also determines that the microfiber optics as a gas sensor used to sense the sensitivity.

4.2.7 Results for sensitivity and linearity of the microfiber optics performance as a gas sensor in different CO2 concentrations

Table 4.11 Sensitivity and linearity of the microfiber optics in different concentrations

Percentage of CO2 gas released	At wavelength 1550nm		At wavelength 1310nm	
	Sensitivity (dBm)	Linearity (%)	Sensitivity (dBm)	Linearity (%)
10%	-0.0143	59.33	-0.0568	76.14
20%	-0.0222	59.19	-0.0735	74.26
30%	-0.1837	73.58	-0.0698	73.26
40%	-0.027	77.51	-0.0717	78.05
50%	-0.0568	76.14	-0.0225	72

Based on the table 4.11, it shows sensitivity and linearity for the microfiber optics in different concentrations of CO2 at wavelength 1550nm and 1310nm. The experiment at the percentage of 30% CO2 gas released at wavelength 1550nm showed higher sensitivity value rather than other experiment, where it manages to obtain a reading of -0.1837dBm while in wavelength 1310nm the highest sensitivity at the percentage of 20% which is -0.0735dBm. Moreover, by comparing two values of linearity in two wavelengths, we can completely see that wavelength 1310nm has near to the line which overall value is above 70%, compared to the wavelength 1550nm. In wavelength 1310nm, at the percentage of 40% gas released, it has the greatest linearity value which 78.05% that resulting in the data fitting in the linear graph. Based on above table, it can be conclude that, at the percentage of 40% CO2 gas released has a perfect correlation interacting with the light source passing through it.

4.2.8 Percentage of CO2 gas released in 1 minutes at different concentrations.

The analysis is based on the sensitivity and linearity percentage of the performance on microfiber optics as a gas sensor in different CO2 concentrations that were carried out.

Through this analysis, the output power have been observed and recorded for every concentration using different wavelengths. This analysis are focused more on performance of the sensor's sensitivity to time as shown in Table 4.12. The first release was about 10% CO2 gas, followed by around 20% and 30% and above.

Table 4.12 Data collected for the experiment time (minutes) vs power meter (dBm)

Percentage of CO2 gas released	Percentage of CO2 gas released in 1 minutes	
	At wavelength 1550nm	At wavelength 1310nm
10%	-37.01	-41.84
20%	-36.57	-40.48
30%	-38.29	-44.47
40%	-36.53	-44.48
50%	-41.84	-40.53

Table 4.13 Sensitivity and linearity of CO2 gas released over time

	Percentage of CO2 gas released in 1 minutes	
	At wavelength 1550nm	At wavelength 1310nm
Sensitivity (dBm)	-9.62	-1.38
Linearity %	68.01	10.86

Through this analysis, the reading value in power (dBm) will be recorded in 1 minutes. This cycle continued three times for every concentration, which helped to reduce random error during data observation. At a wavelength 1550nm, the sensitivity value showed much higher with -9.62dBm where at the wavelength 1310nm is only -1.38dBm. The linearity data at a wavelength 1550nm, showed some magnificent values that can have 68.01 rather than at a wavelength 1310n as shown in Table 4.13. By these results, the sensitivity towards sensor over time be in condition at wavelength 1550nm. However, these sensitivity and linearity results were collected from transmitted power reading. In comparison, we can clearly see that at the wavelengths between 1550nm and 1310nm, the wavelength 1550nm

71

has the greatest linearity that resulting the data to fit in the linear graph. Therefore, the sensitivity and linearity defined by the slope value of wavelength towards a different concentrations of CO2.

Figure 4.7 Percentage of CO2 gas released in 1 minutes

Based on Figure 4.7, shows two different lines for sensitivity with the total outcome in 1 minutes of different CO2 concentrations at 1550nm and 1310nm wavelengths. Each experiment has been checked every 1 minute for a total of 5 minutes at wavelengths 1550nm and 1310nm, with the output measured in decibels (dBm). The optical microfiber acts as a sensor to detect the CO2 gas and perform in different concentrations using different wavelengths. Sensitivity and linearity were used as observed parameters. There is a distinct tendency where the cycle will go up and down before returning to its initial value. This experiment determines that at a wavelength of 1550nm, there is strong positive linear correlation between time and power (dBm). As the time increase, the power also increase. This experiment shows that the optical microfiber sensor has better performance which the sensor is more sensitive to time.

72

4.2.9   Percentage of CO2 gas released in 2 minutes at different concentrations

The analysis is based on the sensitivity and linearity percentage of the performance on microfiber optics as a gas sensor in different CO2 concentrations that were carried out. Through this analysis, the output power have been observed and recorded for every concentration using different wavelengths. This analysis are focused more on performance of the sensor's sensitivity to time as shown in Table 4.14. The first release was about 10% CO2 gas, followed by around 20% and 30% and above.

Table 4.14 Data collected for the experiment time (minutes) vs power meter (dBm)

Percentage of CO2 gas released	Percentage of CO2 gas released in 2 minutes	
	At wavelength 1550nm	At wavelength 1310nm
10%	-37.19	-41.84
20%	-36.85	-40.48
30%	-39.5	-44.73
40%	-36.53	-44.59
50%	-41.84	-40.61

Table 4.15 Sensitivity and linearity of CO2 gas released over time

	Percentage of CO2 gas released in 2 minutes	
	At wavelength 1550nm	At wavelength 1310nm
Sensitivity (dBm)	-8.98	-1.65
Linearity %	62.86	12.49

Through this analysis, the reading value in power (dBm) will be recorded in 2 minutes. This cycle continued three times for every concentration, which helped to reduce random error during data observation. At a wavelength 1550nm, the sensitivity value showed much higher with -8.98dBm where at the wavelength 1310nm is only -1.65dBm. The linearity data at a wavelength 1550nm, showed some magnificent values that can have 62.86

73

rather than at a wavelength 1310nm as shown in Table 4.15. By these results, the sensitivity towards sensor over time be in condition at wavelength 1550nm. However, these sensitivity and linearity results were collected from transmitted power reading. In comparison, we can clearly see that at the wavelengths between 1550nm and 1310nm, the wavelength 1550nm has the greatest linearity that resulting the data to fit in the linear graph. Therefore, the sensitivity and linearity defined by the slope value of wavelength towards a different concentrations of CO2.
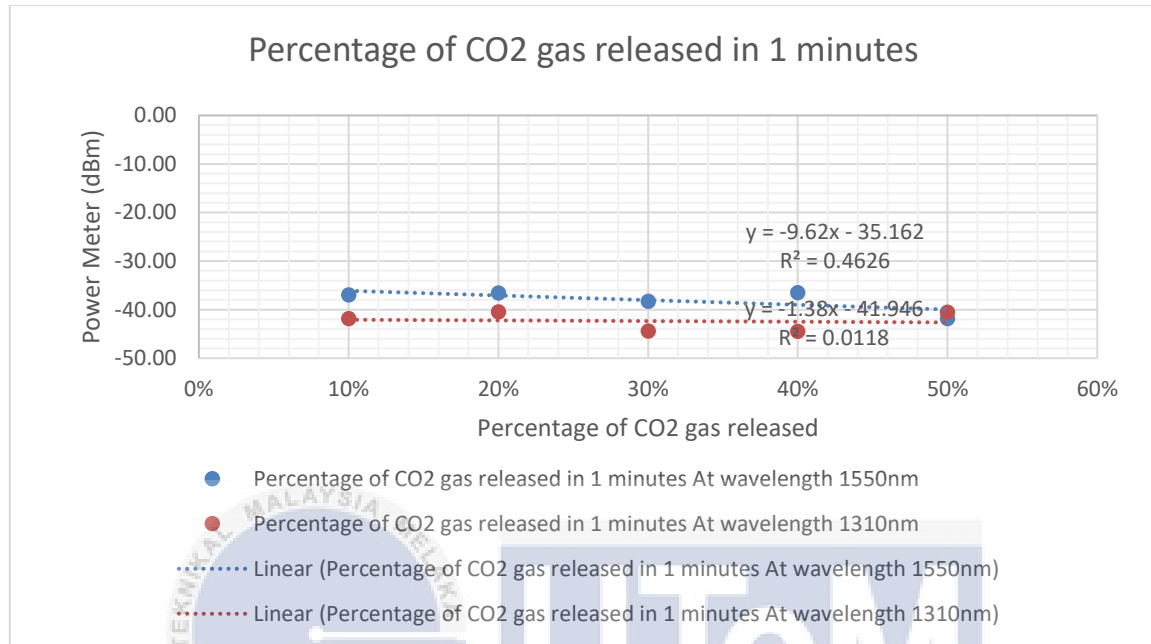

Figure 4.8 Percentage of CO2 gas released in 2 minutes

Based on Figure 4.8, shows two different lines for sensitivity with the total outcome in 2 minutes of different CO2 concentrations at 1550nm and 1310nm wavelengths. Each experiment has been checked every 2 minute for a total of 5 minutes at wavelengths 1550nm and 1310nm, with the output measured in decibels (dBm). The optical microfiber acts as a sensor to detect the CO2 gas and perform in different concentrations using different wavelengths. Sensitivity and linearity were used as observed parameters. There is a distinct tendency where the cycle will go up and down before returning to its initial value. This

74

experiment determines that at a wavelength of 1550nm, there is strong positive linear correlation between time and power (dBm). As the time increase, the power also increase. This experiment shows that the optical microfiber sensor has better performance which the sensor is more sensitive to time.

4.2.10 Percentage of CO2 gas released in 3 minutes at different concentrations

The analysis is based on the sensitivity and linearity percentage of the performance on microfiber optics as a gas sensor in different CO2 concentrations that were carried out. Through this analysis, the output power have been observed and recorded for every concentration using different wavelengths. This analysis are focused more on performance of the sensor's sensitivity to time as shown in Table 4.16. The first release was about 10% CO2 gas, followed by around 20% and 30% and above.

Table 4.16 Data collected for the experiment time (minutes) vs power meter (dBm)

Percentage of CO2 gas released	Percentage of CO2 gas released in 3 minutes	
	At wavelength 1550nm	At wavelength 1310nm
10%	-37.21	-42.25
20%	-36.88	-41.07
30%	-40.14	-45.15
40%	-36.71	-45
50%	-42.25	-40.76

Table 4.17 Sensitivity and linearity of CO2 gas released over time

	Percentage of CO2 gas released in 3 minutes	
	At wavelength 1550nm	At wavelength 1310nm
Sensitivity (dBm)	-9.91	-0.95
Linearity %	63.77	7.14

Through this analysis, the reading value in power (dBm) will be recorded in 3 minutes. This cycle continued three times for every concentration, which helped to reduce random error during data observation. At a wavelength 1550nm, the sensitivity value showed much higher with -9.91dBm where at the wavelength 1310nm is only -0.95dBm. The linearity data at a wavelength 1550nm, showed some magnificent values that can have 63.77 rather than at a wavelength 1310nm as shown in Table 4.17. By these results, the sensitivity towards sensor over time be in condition at wavelength 1550nm. However, these sensitivity and linearity results were collected from transmitted power reading. In comparison, we can clearly see that at the wavelengths between 1550nm and 1310nm, the wavelength 1550nm has the greatest linearity that resulting the data to fit in the linear graph. Therefore, the sensitivity and linearity defined by the slope value of wavelength towards a different concentrations of CO_2.
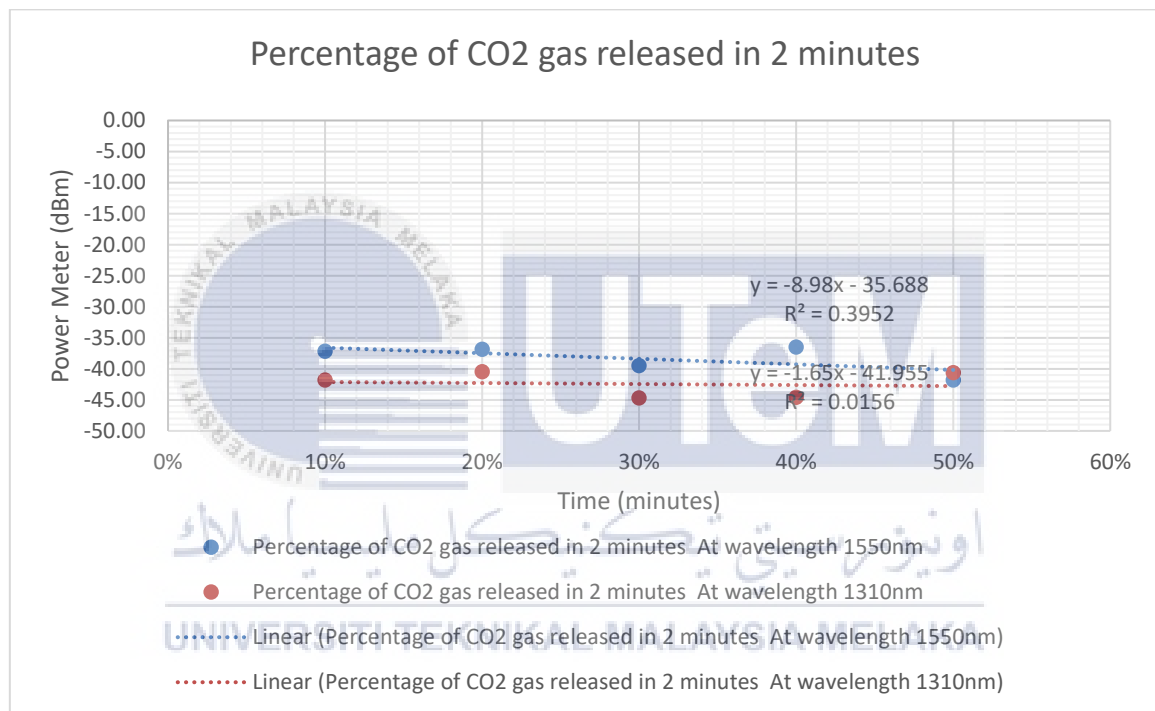

Figure 4.9 Percentage of CO2 gas released in 3 minutes

Based on Figure 4.9, shows two different lines for sensitivity with the total outcome in 3 minutes of different CO2 concentrations at 1550nm and 1310nm wavelengths. Each

experiment has been checked every 3 minute for a total of 5 minutes at wavelengths 1550nm and 1310nm, with the output measured in decibels (dBm). The optical microfiber acts as a sensor to detect the CO2 gas and perform in different concentrations using different wavelengths. Sensitivity and linearity were used as observed parameters. There is a distinct tendency where the cycle will go up and down before returning to its initial value. This experiment determines that at a wavelength of 1550nm, there is strong positive linear correlation between time and power (dBm). As the time increase, the power also increase. This experiment shows that the optical microfiber sensor has better performance which the sensor is more sensitive to time.

4.2.11 Percentage og CO2 gas released in 4 minutes at different concentrations

The analysis is based on the sensitivity and linearity percentage of the performance on microfiber optics as a gas sensor in different CO2 concentrations that were carried out. Through this analysis, the output power have been observed and recorded for every concentration using different wavelengths. This analysis are focused more on performance of the sensor's sensitivity to time as shown in Table 4.18. The first release was about 10% CO2 gas, followed by around 20% and 30% and above.

Table 4.18 Data collected for the experiment time (minutes) vs power meter (dBm)

Percentage of CO2 gas released	Percentage of CO2 gas released in 4 minutes	
	At wavelength 1550nm	At wavelength 1310nm
10%	-37.21	-42.31
20%	-36.88	-41.09
30%	-40.24	-45.18
40%	-36.75	-45.11
50%	-42.31	-40.76

Table 4.19 Sensitivity and linearity of CO2 gas released over time

	Percentage of CO2 gas released in 4 minutes	
	At wavelength 1550nm	At wavelength 1310nm
Sensitivity (dBm)	-10.07	-0.92
Linearity %	64.02	6.78

Through this analysis, the reading value in power (dBm) will be recorded in 4 minutes. This cycle continued three times for every concentration, which helped to reduce random error during data observation. At a wavelength 1550nm, the sensitivity value showed much higher with -10.07dBm where at the wavelength 1310nm is only -0.92dBm. The linearity data at a wavelength 1550nm, showed some magnificent values that can have 64.02 rather than at a wavelength 1310nm as shown in Table 4.19. By these results, the sensitivity towards sensor over time be in condition at wavelength 1550nm. However, these sensitivity and linearity results were collected from transmitted power reading. In comparison, we can clearly see that at the wavelengths between 1550nm and 1310nm, the wavelength 1550nm has the greatest linearity that resulting the data to fit in the linear graph. Therefore, the sensitivity and linearity defined by the slope value of wavelength towards a different concentrations of CO2.
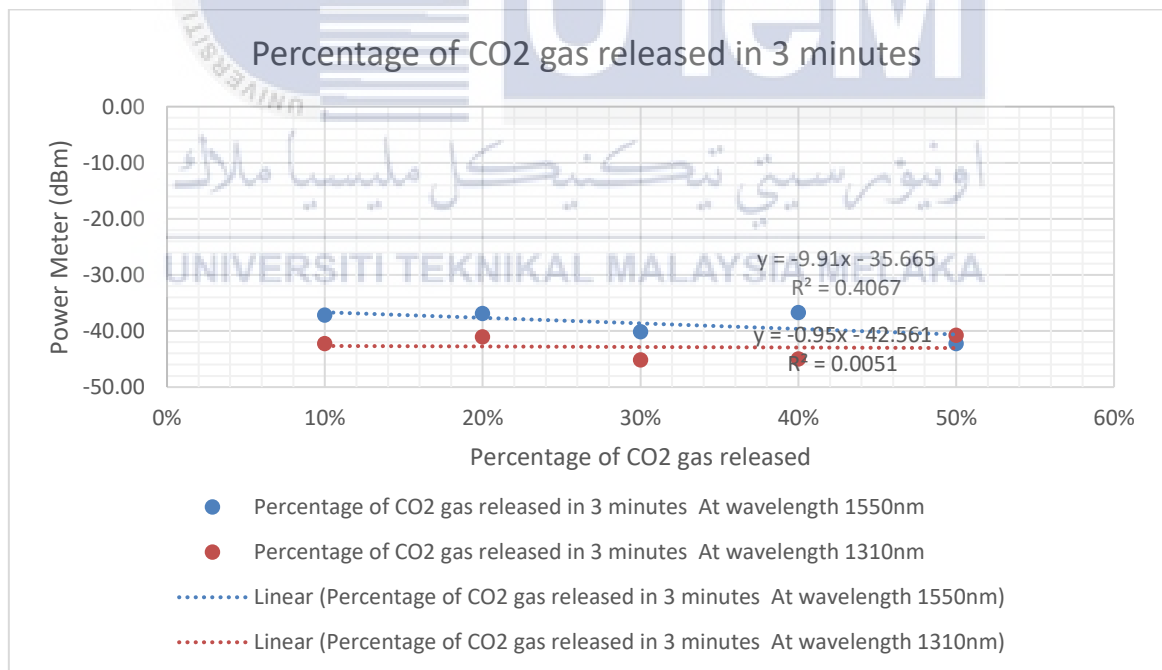
Figure 4.10 Percentage of CO2 gas released in 4 minutes

Based on Figure 4.10, shows two different lines for sensitivity with the total outcome in 4 minutes of different CO2 concentrations at 1550nm and 1310nm wavelengths. Each experiment has been checked every 4 minute for a total of 5 minutes at wavelengths 1550nm and 1310nm, with the output measured in decibels (dBm). The optical microfiber acts as a sensor to detect the CO2 gas and perform in different concentrations using different wavelengths. Sensitivity and linearity were used as observed parameters. There is a distinct tendency where the cycle will go up and down before returning to its initial value. This experiment determines that at a wavelength of 1550nm, there is strong positive linear correlation between time and power (dBm). As the time increase, the power also increase. This experiment shows that the optical microfiber sensor has better performance which the sensor is more sensitive to time.

79

4.2.12 Percentage of CO2 gas released in 5 minutes at different concentrations

For this analysis is based on the sensitivity and linearity percentage of the performance on microfiber optics as a gas sensor in different CO2 concentrations that was carried out during the test. Through these analysis the output power have been observed and recorded for every concentration by using a different of wavelength. In this analysis are focused more on performance of the sensor's sensitivity to time as shown in Table 4.20. For the first released was about 10% of CO2 gas then following around 20% and 30% and above.

Table 4.20 Data collected for the experiment time (minutes) vs power meter (dBm)

Percentage of CO2 gas released	Percentage of CO2 gas released in 5 minutes	
	At wavelength 1550nm	At wavelength 1310nm
10%	-37.21	-42.31
20%	-36.88	-41.1
30%	-40.29	-45.19
40%	-36.75	-45.12
50%	-42.31	-40.76

Table 4.21 Sensitivity and linearity of CO2 gas released over time

	Percentage of CO2 gas released in 5 minutes	
	At wavelength 1550nm	At wavelength 1310nm
Sensitivity (dBm)	-10.07	-0.92
Linearity %	63.82	6.78

Through The experiment repeated three cycles for each different concentrations in CO2, which helps to reduce random error during data collections. At a wavelength 1550nm, the sensitivity value showed much higher with -10.07dBm where at the wavelength 1310nm is only -0.92dBm. The linearity data at a wavelength 1550nm, showed some magnificent values that can have 63.82 rather than at a wavelength 1310nm as shown in Table 4.21. By

these results, the sensitivity towards sensor over time be in condition at wavelength 1550nm. However, these sensitivity and linearity results were collected from transmitted power reading. In comparison, we can clearly see that at the wavelengths between 1550nm and 1310nm, the wavelength 1550nm has the greatest linearity that resulting the data to fit in the linear graph. Therefore, the sensitivity and linearity defined by the slope value of wavelength towards a different concentrations of CO2.
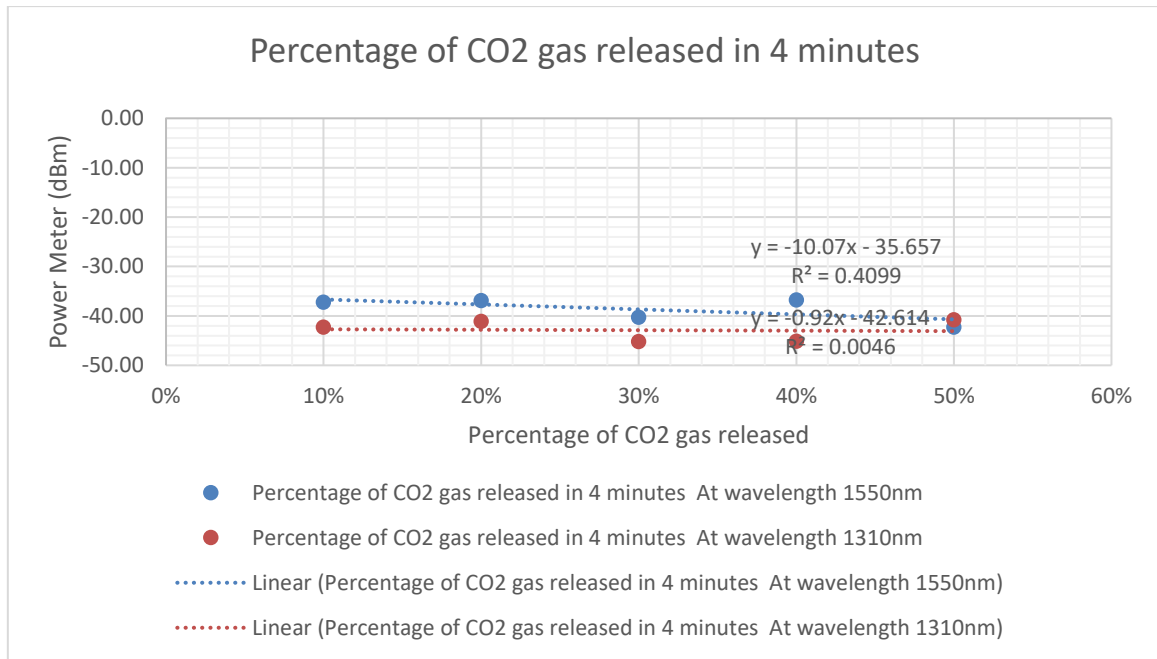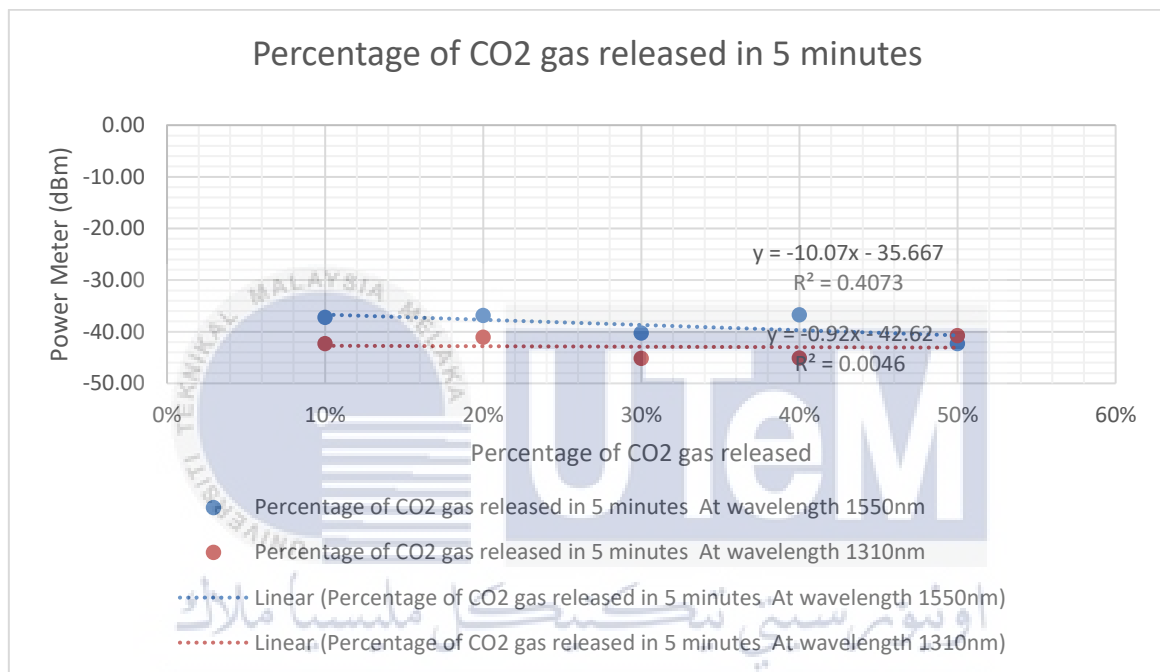

Figure 4.11 Percentage of CO2 gas released in 5 minutes

Based on Figure 4.11, shows two different lines for sensitivity with the total outcome in 4 minutes of different CO2 concentrations at 1550nm and 1310nm wavelengths. Each experiment has been checked every 5 minute for a total of 5 minutes at wavelengths 1550nm and 1310nm, with the output measured in decibels (dBm). The optical microfiber acts as a sensor to detect the CO2 gas and perform in different concentrations using different wavelengths. Sensitivity and linearity were used as observed parameters. There is a distinct tendency where the cycle will go up and down before returning to its initial value. This experiment determines that at a wavelength of 1550nm, there is strong positive linear

81

correlation between time and power (dBm). As the time increase, the power also increase. This experiment shows that the optical microfiber sensor has better performance which the sensor is more sensitive to time.

4.2.13 Results sensitivity and linearity for percentage of CO2 gas released in time (minutes) at different concentrations.

Table 4.22 Sensitivity and linearity for percentage of CO2 gas released in time (minutes) at different concentrations.

Time (minutes)	At wavelength 1550nm		At wavelength 1310nm	
	Sensitivity (dBm)	Linearity (%)	Sensitivity (dBm)	Linearity (%)
1	-9.62	68.01	-1.38	10.86
2	-8.98	62.86	-1.65	12.49
3	-9.91	63.77	-0.95	7.14
4	-10.07	64.02	-0.92	6.78
5	-10.07	63.82	-0.92	6.78

Based on the table 4.22, it shows the time taken for the sensitivity and linearity of microfiber optics in different CO2 concentrations at wavelengths of 1550nm and 1310nm. Experiments in four and five minutes at a wavelength of 1550nm showed the same and higher sensitivity values compared to others, where it managed to obtain a reading of -10.07dBm while in wavelength of 1310nm the highest in the second minute was -1.65dBm. In addition, by comparing the two linearity values in the two wavelengths, we can completely see that wavelength 1550nm has near to the line which overall value is above 60%, compared to the 1310nm wavelength. In the wavelength of 1550nm, time in 1 minute has the greatest linearity value which 68.01% that resulting the data to fit in the linear graph. Based on above table, we can conclude that, in the first minute the CO2 gas released has a perfect correlation that interacts with the light source that passes through it. This shows that the optical microfiber sensor has a better performance where the sensor is more sensitive to time.

4.3　Summary

This chapter presented case studies to demonstrate applicability of the proposed microfiber optic sensor development system in different concentrations of CO2 using a tapering method. The case study is based on five samples different concentrations of CO2 tested. The CO2 gas is released three times for the first, and it was released about 10% of CO2 gas then following around 20% and 30% and above. Through these analysis the output power have been observed and recorded for every concentrations by using a different of input wavelength. The performance as microfiber optics gas sensor at different wavelengths, were defined to be well performed by sensitivity and linearity results analysis. However, the linear graph slope were determined as sensitivity value in different CO2 concentrations. The experiment repeated by three time cycle to reduce random reading error to ensure data collection accuracy.
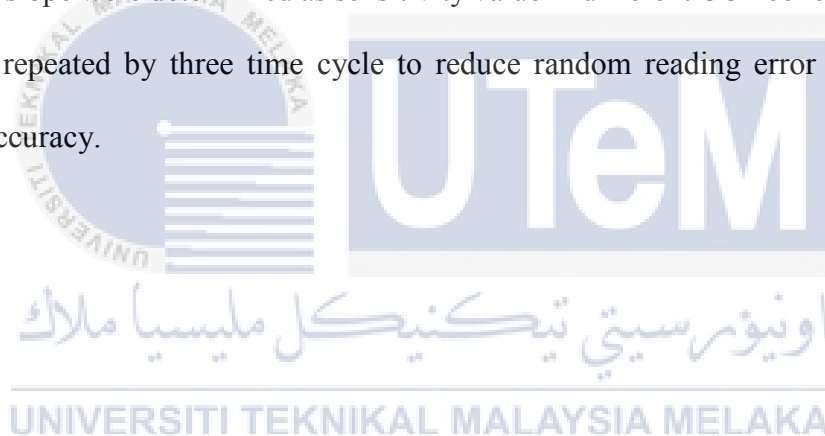
CHAPTER 5

CONCLUSION AND RECOMMENDATIONS

5.1   Conclusion

The method for developing microfiber optic sensors for CO2 in different concentrations using a tapering method is presented in this thesis. The proposed methodology is effective and robust for obtaining good results with only precise data and minimal network measurement information. The proposed analytical method of obtaining the correlation for each samples of different concentrations in CO2 by combining sensitivity and linearity. The analysis of the sensor throughout the measurement showed that it has good stability of the measurement at small change of concentration. In addition, microfiber sensors have shown special advantages such as high sensitivity for refractive index measurement over conventional optical fiber sensors due to their small sizes and high-fractional evanescent fields. Furthermore, the tight confinement and surface enhancement of probing light waveguided along a microfiber are advantageous for achieving high-sensitivity with low optical power, which is highly desired for many applications.

Overall, the study provided in this thesis has contributed to a better understanding of sensor relevance in microfiber optics. The presented method makes good use of a restricted amount and type of data, uses simple mathematical manipulations, and requires fewer intensive calculations while producing quick, compelling, reflective, and accurate results. The research focused on developing approaches that would aid in the development of low-cost sensors that are solely dependent on optical microfiber sensing. As a result, it paves the way for the recommended extra research.

84

5.2 Future Works

For future improvements, there are a number of oppurtunities and recommendations for microfiber optical sensing including:

i) Using microfiber optic sensor to measure other variables such as temperature, pressure, and humidity. Because the main construction of both sensors is glass and they are resistant to harmful interference such as electromagnetic interference (EMI) and can tolerate harsh condition such as high temperature and pressure.

ii) For even greater ease and convenience in monitoring sensor output, microfiber optic sensors can be linked to the Internet of Things (IoT). IoT enables remote monitoring since authorized users may access the system from anywhere in the global. Additionally, extending the detecting zone might boost sensor sensitivity that the sensors may provide a greater resonant output whwn a optical signal passes through it.

iii) The microfiber optical sensors can be formed in any shape such as D-shape and microbottle resonators. It is because of their cost-effective and attractive due to their inherent advantages such as the immunity to electromagnetic interference, compact size, and lightweight.

iv) These optical microfiber gas sensor using a tapering method, have shown potential applications in highly-sensitive gas sensing in combining with microfiber and new materials.

REFERENCES

[1] Mohd Hafiz Jali, Hazli Rafis Abdul Rahim, Md Ashadi Md Johari, Haziezol Helmi Mohd Yusof, Aminah Ahmad, Siddharth Thokchom, Kaharudin Dimyati, Sulaiman Wadi Harun, "Humidity sensing using microfiber-ZnO nanorods coated glass structure," *Optik,* 2021.

[2] Chen G Y, Ding M, Newson T and Brambilla G, "A review of microfiber and nanofiber based optical sensors," *The Open Optics Journal,* 2013.

[3] Jin-hui Chen, Dan-ran Li and Fei Xu, "Optical Microfiber Sensors: Sensing Mechanisms, and Recent Advances," *Journal of Lightwave Technology,* 2018.

[4] Tang J, Zhou J, Guan J, Long S, Yu J, Guan H, Lu H, Luo Y, Zhang J and Chen Z, "Fabrication of side-polished single mode-multimode-single mode fiber and its characteristics of refractive index sensing," *IEEE Journal of Selected Topics in Quantum Electronics,* 2017.

[5] T. Zhu, D. Wu, M. Liu, and D. W. Duan, "In-line fiber optic interferometric sensors in single-mode fibers," *Sensors,* jld. 12, 2012.

[6] Prachi Sharma, Suraj Pardeshi, Rohit Kumar Arora, Mandeep Singh, "A Review of the Development in the Field of Fiber Optic Communication Systems," *International Journal of Emerging Technology and Advanced Engineering,* jld. 3, no. 5, 2013.

[7] B. Srinivasan and D. Venkitesh, "Distributed fiber-optic sensors and their applications," *Opt. Fiber Sensors Adv. Tech,* 2017.

[8] S. Zhang, H. Liu, A. A. S. Coulibaly, and M.DeJong, "Fiber Optic Sensing of concrete cracking and rebar deformation using several types of cable," *Struct Control Heal Monit,* jld. 28, 2021.

[9] N.I.Zanoon, "The Phenomenon of Total Internal Refkection and Acceleration of Light in Fiber Optics," *Int. J. Comput. Appl,* jld. 107, pp. 19-24, 2014.

[10] M. Loyez et al., "Rapid Detection of Circulating Breast Cancer Cells Using a Multiresonant Optical Fiber Aptasensor with Plasmonic Amplification," *ACS Sensors,* jld. 5, pp. 454-463, 2020.

[11] A.Acakpovi and Matoumana, "Comaparative analysis of plastic optical fiber and glass optical fiber for home networks," *IEEE 4th Int. Conf. Adapt. Sci. Technol,* pp. 154-157, 2012.

[12] G. Brambilla, "Optical fibre nanowires and microwires: a review," *Journal of Optics,* 2010.

[13] Kok-Sing Lim, Hamzah Arof, Sulaiman Wadi Harun, H. Ahmad, "Fabrication and Applications of Microfiber," *Selected Topics on Optical Fiber Technology,* 2018.

[14] Mohd Hafiz Jali et al, "Optical Microfiber Sensor: A Review," *Journal of Physics: Conference Series,* 2021.

[15] Wu X and Tong L, "Optical microfibers and nanofibers," *Nanophotonics,* no. 2, pp. 28-51, 2018.

[16] Xiaoqin Wu and Limin Tong, "Optical microfibers and nanofibers," *Nanophotonics,* 2013.

[17] Brambilla, Gilberto, "Optical fibre nanotaper sensors," *Optical Fiber Technology,* 2010.

[18] Guo X and Tong L , "Supported microfiber loops for optical sensing," *Optics Express,* 2017.

[19] Xu F and Brambilla G J A P L, "Demonstration of a refractometric sensor based on optical microfiber coil resonator," *Sensors,* jld. 5, 2019.

[20] Fan X, White I M, Shopova S I, Zhu H, Suter J D and Sun Y J a c a, "Sensitive Optical Biosensors for unlabeled targets: A review," 2019.

[21] Tong LM, Zi F, Guo X, Lou JY, "Optical Microfibers and nanofibers: A Tutorial," *Opt Commun,* pp. 7-64, 2012.

[22] H. Segawa, E. Ohnishi, Y. Arai, and K. Yoshida, "Sensitivity of fiber-optic carbon dioxide sensors utilizing indicator dye," *Sensors Actuators B Chem,* jld. 94, 2013.

[23] C. S. Chu and Y. L. Lo, "Highly sensitive and linear optical fiber carbon dioxide sensor based on sol-gel matrix doped with silica particles and HPTS," *Sensors Actuators B Chem,* jld. 143, 2019.

[24] A. Ksendzov, S. Forouhar, R. M. Briggs, C. Frez, K. J. Franz, and M. Bagheri, "Linewidth measurement of high power diode laser at 2μm for carbon dioxide detection," *Electron,* jld. 48, 2016.

[25] J. A. Nwaboh, J. Hald, J. K. Lyngso, J. C. Petersen, and O. Werhahn, "Measurements of CO2 in a multipass cell and in a hollow-core photonic bandgap fiber at 2 μm,," *Appl. Phys. B,* jld. 110, 2016.

[26] S. Pevec and D. Donlagic, "Nanowire-based refractive index sensor on the tip of an optical fiber," *Appl. Phys. Lett.,* jld. 102, 2013.

[27] B. N. Shivananju, S. Yamdagni, R. Fazuldeen, A. K. Sarin Kumar, G. M. Hegde, M., "CO2 sensing at room temperature using carbon nanotubes," *Rev. Sci. Instrum,* jld. 84, 2013.

[28] X. Chong, K. J. Kim, P. R. Ohodnicki, E. Li, C. H. Chang, and A. X. Wang, "Ultrashort Near-Infrared Fiber-Optic Sensors for Carbon Dioxide Detection," *IEEE Sens. J.,* jld. 15, 2015.

[29] R. Orghici, U. Willer, M. Gierszewska, S. R. Waldvogel, and W. Schade, "Detection of explosives and CO2 dissolved in water with an evanescent field sensor," *Conf. Quantum Electron. Laser Sci. Conf. Lasers Electro-Optics,* 2018.

[30] M. V. Avdeev, A. N. Konovalov, V. N. Bagratashvili, V. K. Popov, S. I. Tsypina, M. Sokolova, J. Ke, and M. Poliakoff, "The fibre optic reflectometer: A new and simple probe for refractive index and phase separation measurements in gases, liquids and supercritical fluids," *Phys. Chem. Chem. Phys,* jld. 6, 2011.

[31] X. D. Wang and O. S. Wolfbeis, "Fiber-Optic Chemical Sensors and Biosensors," *Anal. Chem,* jld. 88, 2016.

[32] J. Villatoro, D. Monzón-Hernández, and D. Talavera, "High resolution refractive index sensing with cladded multimode tapered optical fibre," *Electron. Lett,* jld. 40, 2011.

[33] Nasir, M.N.M., G.S. Murugan, and M.N. Zervas, "Broadly tunable solid microbottle resonator," *In photonics conference (IPC). IEEE,* 2016.

Appendix A   Gantt Chart for BDP 1

NO	TITLE	(BDP 1) SEM 2 2022/2023													
		1	2	3	4	5	6	7	8	9	10	11	12	13	14
1	Title selection and BDP Registration	▨													
2	Background study: Search for papers related to the project		▨	▨											
3	Evaluate of Work Progress 1														
4	Complete report for Chapter 1 (Introduction)														
5	Complete report for Chapter 2 (Literature Review)									▨					
6	Complete report for Chapter 3 (Methodology)										▨				
7	Evaluate of Work Progress 2												▨		
8	Submit report with turnitin <30%													▨	
9	BDP 1 Presentation														▨
10	Submission and evaluation of BDP 1 final report on ePSM report														▨

Column 8: MID TERM BREAK

Appendix B   Gantt Chart for BDP 2

NO.	TITLE	(BDP 2) SEM 2 2022/2023													
		1	2	3	4	5	6	7	8	9	10	11	12	13	14
1	Continue with study while start the project: Search for papers related to the project, stripping the fiber, splicing fiber with connector input and output		▨	▨	▨	▨	▨								
2	Evaluate of Work Progress 1								MID TERM BREAK						
3	Start working on the project: Stripping the fiber, Splicing and Tapering												▨		
4	Complete report for Chapter 4 (Results)												▨		
5	Collect data results, conclusion, and draft report						▨						▨		
6	Evaluate of Work Progress 2												▨		
7	Submit first draft report to SV, report correction													▨	
8	Submit report with turnitin <30%													▨	
9	BDP 2 Presentation														▨
10	Submission and evaluation of BDP 1 final report on ePSM report														▨